Book Chapter

Mn-Based MRI Contrast Agents: An Overview

Céline Henoumont[1], Marie Devreux[1] and Sophie Laurent[1,2]*

[1]NMR and Molecular Imaging Laboratory, Department of General, Organic and Biomedical Chemistry, University of Mons, 19 Avenue Maistriau, 7000 Mons, Belgium
[2]Center for Microscopy and Molecular Imaging (CMMI), 8 Rue Adrienne Boland, 6041 Gosselies, Belgium

***Corresponding Author:** Sophie Laurent, NMR and Molecular Imaging Laboratory, Department of General, Organic and Biomedical Chemistry, University of Mons, 19 Avenue Maistriau, 7000 Mons, Belgium

Published **January 29, 2024**

This Book Chapter is a republication of an article published by Sophie Laurent, et al. at Molecules in October 2023. (Henoumont, C.; Devreux, M.; Laurent, S. Mn-Based MRI Contrast Agents: An Overview. Molecules 2023, 28, 7275. https://doi.org/10.3390/molecules28217275)

How to cite this book chapter: Céline Henoumont, Marie Devreux and Sophie Laurent. Mn-Based MRI Contrast Agents: An Overview. In: Noor Zarina Abd Wahab editor. Prime Archives in Molecular Sciences: 4th Edition. Hyderabad, India: Vide Leaf. 2024.

Acknowledgements: This work was performed with the financial support of the Walloon Region, FNRS, and the COST actions. Authors thank the Center for Microscopy and Molecular Imaging (CMMI, supported by European Regional Development Fund and Wallonia).

Conflict of Interest: The authors declare no conflict of interest.

Abstract

MRI contrast agents are required in clinic to detect some pathologies, such as cancers. Nevertheless, at the moment, only small extracellular and non-specific gadolinium complexes are available for the clinicians. Moreover, safety issues have recently appeared concerning the use of gadolinium complexes, so that alternatives are urgently needed. Manganese-based MRI contrast agents could be one of these alternatives and more and more studies are available in the literature. This review aims at synthesizing all those researches, from small Mn-complexes to nanoparticular agents, including theranostic agents, to highlight all the efforts already made by the scientific community to obtain highly efficient agents, but also evidence the weaknesses of the developed systems.

Keywords

Mn-Complexes; Mn-based Nanoparticles; Theranostic; Magnetic Resonance Imaging

Graphical Abstract

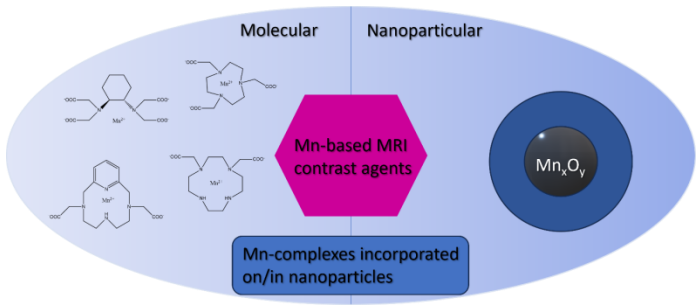

Introduction

Medical diagnosis by Magnetic Resonance Imaging (MRI) often requires the use of contrast agents to highlights some pathological regions, such as tumor tissues. Gadolinium complexes are currently the most utilized contrast agents in the clinical field thanks to their property to enhance the water proton longitudinal relaxation [1]. Nevertheless, since many years, it has been demonstrated that the injection of gadolinium complexes to patients with kidneys failure is responsible of the apparition of a disease called nephrogenic systemic fibrosis (NSF) [2-5]. It has been particularly evidenced for linear gadolinium complexes based on acyclic ligands such as Gd-DTPA (gadopentetic acid) since they are less thermodynamically and kinetically stable than those based on macrocyclic complexes such as Gd-DOTA (gadoteric acid). Therefore, those acyclic Gd-based CAs (GBCAs) are no longer recommended for those patients [2,3,6]. Additionally, more recent studies have demonstrated an accumulation of gadolinium CAs in the brain of subjects with normal renal function [5-10]. This situation has attracted researches on Gd-free alternatives, among which we can cite the development of magnetic nanoparticles [11], of fluorine MRI [12], of non-metal nitroxide radical based systems [13], or of manganese-based CAs on which this review will focus [14-16]. Manganese ions can be found in the body under the form Mn^{2+} or Mn^{3+} with 5 or 4 unpaired d-orbital electrons, respectively. Its normal physiological concentration in the serum of healthy subjects is about 0.5–1.2 µg/dL (9–22 µM), and it will work in the organism as a cofactor activating some enzymes or as a constituent in metalloenzymes. Manganese ions also act in the development of the immune and nerve system functions and in the regulation of vitamins and sugar in the blood [17,18]. Mn-based MRI contrast agents were first used as an oral formulation containing liposome-encapsulated $MnCl_2$ salt (LumenHance®), indicated for gastrointestinal images. Nevertheless, it was shown that too high doses of free manganese ions could induce a neurodegenerative disorder called manganism, a disease with symptoms similar to those of the Parkinson's disease. This contrast agent is therefore no longer used, but manganese enhanced MRI (MEMRI) using

$MnCl_2$ is still utilized for preclinical studies in mice with brain [19] or lung [20] model tumors. For a safety use in clinic, manganese complexes have been developed, and the second manganese-based CA approved by the Food and Drug Administration (FDA) in 1997 was manganese dipyridoxyl diphosphate (Mn-DPDP, Teslascan®, figure 1) for use as a liver specific hepatobiliary CA [21,22]. Nevertheless, its efficacy was quite limited and some toxicity issues were evidenced due to the release of free Mn ions in vivo. As a result, Mn-DPDP is no longer commercialized for clinical use, so that there is still a need for Gd-free alternatives, with a high thermodynamic stability and kinetic inertness, and with a high efficacy to be competitive with GBCAs [14-16,23]. This review aims at synthesizing the actually developed Mn-based MRI contrast agents since more and more researches are conducted on this subject with a high diversity on the proposed structures, but a unique goal: the ability for the Mn-agents to reach their target at a low dose and to produce a sufficiently high MRI signal.

Molecular Mn-based Contrast Agents

Similarly to the Gd-complexes, the efficacy of molecular Mn-based contrast agents is based on the presence of at least one exchanging water molecule in the inner coordination sphere of the metal, characterized by a fast exchange rate. The typical coordination number of Mn(II) complexes in aqueous solution being 6, 7, or sometimes 8, this innersphere water molecule is assured if the ligand possesses 5 or 6 coordination bonds with the metal. Nevertheless, the thermodynamic stability and the kinetic inertness of Mn-complexes is generally lower than that of Gd-complexes because of the lower charge of Mn ions, and the lack of ligand-field stabilization energy (high spin d^5 electron configuration). Moreover, the possible oxidation of Mn^{2+} to Mn^{3+}, which is often related to the thermodynamic stability of the Mn(II)-complex, has also to be avoided as it will lead to a loss of efficacy because of the loss of one unpaired electron and of a less favorable electronic relaxation. Nevertheless, one example of Mn(III) complexes can be found in the literature [24]. They are based on planar tetradentate chelates assembled from a 1,2-phenylenediamido backbone. Their relaxivity

(defined as the increase of the water proton relaxation rate induced by 1 mmole per liter of the contrast agent) is comparable to that of clinically used Gd-based contrast agents, and they are moreover able to accumulate in intracellular compartments.

Thus, in their efforts to incorporate manganese ions in a stable and efficacious structure, researchers have developed a lot of different ligands to coordinate Mn ions, even linear or cyclic [14-16]. All those developed complexes are even non-specific and rapidly cleared by the kidneys or targeted to specific organs or tissues such as tumors or the liver. Some of them can also be responsive to a certain stimulus or combine several imaging techniques. This will be developed in the following, at the exception of a particular class of ligands, the porphyrins, which allow to incorporate Mn ions in the center of the heme ring. Mn-porphyrins represent a very interesting and promising class of Mn-based contrast agents, characterized by high relaxivities, but they were the object of a recent extensive review [25] so that it is useless to describe them again here.

Non Specific Contrast Agents

Complexes based on Linear Ligands

EDTA (ethylene diamine tetraacetic acid, figure 1) is a linear hexadentate ligand able to form very stable complexes with Mn ions and was thus extensively studied. Indeed, previous works on $[Mn(EDTA)(H_2O)]^{2-}$ have shown that its sodium salt is very well tolerated: LD50 is 7.0 mmol/kg in rats following intravenous injection compared with an LD50 of 0.22 mmol/kg for $MnCl_2$ [26]. It allows moreover the presence of one fast exchanging water molecule, so that the relaxivities of the complexes $[Mn(EDTA)(H_2O)]^{2-}$ and $[Gd(DTPA)(H_2O)]^{2-}$ are similar (2.9 and 4.1 mM^{-1} s^{-1} , respectively at 20 MHz, 35 °C) (table 1) [27]. The increased relaxivity of the Gd(III) complex may be due to its larger size and slower tumbling rate. As it is well-known that a decrease of the tumbling rate can boost the efficacy of the contrast agents, several studies have tried to increase the size of the Mn-complex. We can cite for example the work of Caravan *et al.* [28] who have grafted six tyrosine-derived $[Mn(EDTA)(H_2O)]^{2-}$ moieties to a cyclotriphosphazene core.

The 37°C per Mn(II) relaxivity ranged from 8.2 to 3.8 mM^{-1} s^{-1} from 0.47 to 11.7 T, and is sixfold higher on a per molecule basis. Other researches were focused on the improvement of the stability of the Mn-complexes based on linear ligands by rigidifying the chelator. We can cite the addition of a cyclohexane ring (Mn-CDTA) [29,30], of one or two pyridine rings (Mn-PyC3A, Mn-PAADA, Mn-DPAA, Mn-DPAMeA or Mn-DPAPhA) [31-36], or of piperidine rings (Mn-AMPTA, or Mn-AMPDA-HB) [37] (figure 1, table 1), forming pentadentate or hexadentate ligands. As expected, pentadentate complexes were globally less stable than hexadentate complexes whereas the increased rigidity of the chelator allowed to obtain more stable complexes. For example, the pMn of Mn-CDTA is higher than that of Mn-EDTA (8.67 for Mn-CDTA versus 7.82 for Mn-EDTA at pH 7.4) [29]. Mn-PyC3A [31-34] can also be cited for its good thermodynamic (pMn of 8.17 at pH 7.4) and kinetic stability, as well as a good relaxivity of 2.1 s^{-1} mM^{-1} at 1.4 T and 37°C (table 1) and it has recently started phase I clinical trials (NCT05413668). It has moreover been demonstrated as a potential alternative to gadolinium to characterize acute myocardial infarctions [38]. In the attempts to increase the stability of the complexes and the kinetic inertness towards endogenous ions such as Zn^{2+} ions, the work of Wadepohl *et al.* [39] opens interesting perspectives. It is based on bispidine derivatives providing rigid and large coordination cavities that perfectly match the size of Mn^{2+} ions.

All those cited complexes often representing difficult synthetic procedures, we can cite to conclude this part the study of Stasiuk *et al.* [40] who are proposing a single-pot template reaction to obtain a Mn-based contrast agent endowed with a good kinetic inertness towards zinc transmetallation and an interesting relaxivity of 5.2 s^{-1} mM^{-1} at 1.5 T and 298 K.

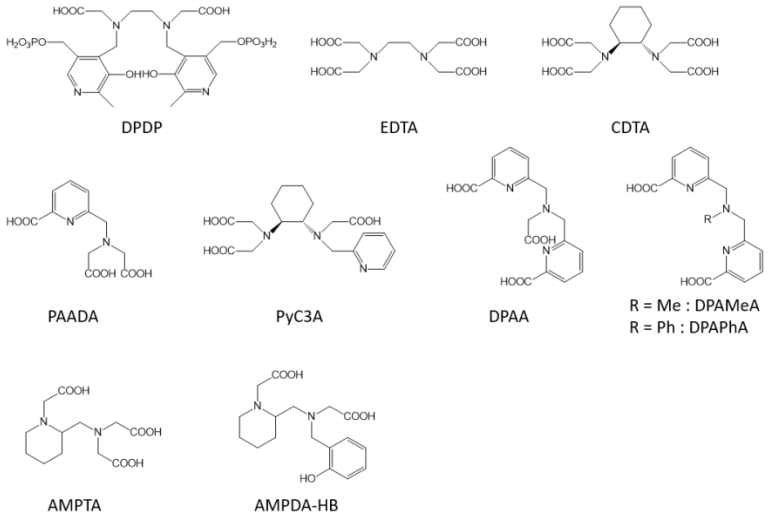

Figure 1: Linear ligands discussed in this work.

Complexes based on Macrocyclic Ligands

Globally, complexes based on macrocyclic ligands are more thermodynamically stable than those based on linear ligands, so that a lot of researches are focused on macrocyclic complexes.

A first well-known category of macrocyclic ligands is the triazacyclononane derivatives. Several studies have shown that hexadentate ligands, such as NOTA (figure 2) [41] or its derivatives where one acetate pendant arm is replaced by other donor groups as a sulfonamide [42], an acetamide [43] or a methylene pyridine group [44], lack the presence of one innersphere water molecule when they are complexed with Mn(II) ions, with consequently very low relaxivities. Rodriguez-Rodriguez *et al.* [43] took advantage of this absence of any innersphere water molecule to study more thoroughly the effect of the electron spin relaxation at low field and they have shown that the electronic relaxation is quite insensitive to the nature of the donor atom but depends more on the coordination polyhedron. Nevertheless, if one of the donor group is replaced by other substituents, pentadentate ligands (1,4,7,-triazacyclononane-1,4-diacetic acid, H_2NO_2A, figure 2, table 1)

allowing the presence of one innersphere water molecule when complexed to Mn(II) ions are obtained. Those complexes were extensively studied [44-48], with a special interest in the more recent study [48] on the water exchange rate, which has to be sufficiently high to assure a good relaxivity. The authors found thanks to ^{17}O measurements and DFT calculations that the water exchange rate is greatly influenced by the bulkiness of the substituent at the position 7 of the triazacyclononane unit.

Similarly to NOTA, the DOTA ligand (figure 2), a well-known tetraazatetradecane ligand, does not allow the presence of one innersphere water molecule when complexed to Mn(II) ions. Nevertheless, as Toth *et al.* [41] have shown a highest kinetic stability towards zinc transmetallation for the Mn-DOTA complex compared to the Mn-NOTA, derivatives of DOTA allowing the presence of one innersphere water molecules could be interesting. Therefore, Mn(II) complexes with cyclen-based ligands bearing one, two and three acetate pendant arms [49,50] (DO1A = 1,4,7,10-tetraazacyclododecane-1-acetic acid, cis- and trans-DO2A (Cis = 1,4,7,10-tetraazacyclododecane-1,4-diacetic acid, Trans = 1,4,7,10-tetraazacyclododecane-1,7-diacetic acid) and DO3A = 1,4,7,10-tetraazacyclododecane-1,4,7-triacetic acid, figure 2) were studied by ^{1}H and ^{17}O relaxometry. The results were the absence of any innersphere water molecule for Mn-DO3A, as well as for Mn-trans-DO2A, whereas Mn-cis-DO2A and Mn-DO1A complexes contain one innersphere water molecule (table 1). It has nevertheless to be noted that the decreased denticity of the ligand results, as expected, in a decrease of the complex stability. Botta *et al.* [51] investigated also the replacement of the acetate by N,N-dimethylacetamides pendant arms (1,4-DO2AM, figure 2, table 1), and they obtained an increased kinetic inertness. This was confirmed by the study of Garda *et al.* [52] who replaced the acetate arms by phosphonate arms, or mono-, secondary-, or tertiary amides arms, and their results point out that phosphonates lead to a decrease of the complex stability, whereas tertiary amides afford encouraging results to increase the stability.

The AAZTA ligand (figure 2) [29] (AAZTA = 6-amino-6-methylperhydro-1,4-diazepine tetraacetic acid) is another macrocyclic chelate able to complex Gd^{3+} and Mn^{2+} ions. Similarly to the case of DOTA, whereas the Gd-AAZTA complex allows the presence of two innersphere water molecules, the Mn-AAZTA complex is characterized by the absence of water co-ligand, so that its relaxivity is quite low. Botta *et al.* [53] have thus synthesized 3 AAZTA derivatives, with only three acetate or α-methylacetate arms (Mn-AAZ3A, Mn-MeAAZ3A and Mn-AAZ3MA, figure 2). Those complexes have one innersphere water molecule and hence a better relaxivity (table 1), but once again to the detriment of the stability (huge decrease of the pMn value for the three derivatives compared to Mn-AAZTA).

Pyclen (3,6,9,15-tetraazabicyclo[9.3.1]pentadeca-1(15),11,13-triene) is another interesting 12-membered macrocyclic structure characterized by a *N*-pyridyl donor that rigidifies and pre-organizes the ligand coordinating groups (in particular rendering the 4 nitrogen atoms coplanar), which could improve the kinetic inertness of the resulting complex. The pyridine subunit also endows the ligand with an increased degree of lipophilicity that could induce mixed renal and hepatobiliary clearances, another interesting advantage in the context of patients with reduced kidney function. The pyclen ([12]PyN4) macrocyclic core is now recognized to form efficient chelators for the Mn^{2+} cation complexation, and some studies can be found on the interest of such pyridine-containing (PC) ligands. Garda *et al.* [52] studied derivatives of PCTA (figure 2), with 3 pendant arms, and studied the influence of the presence of a primary, a secondary or a tertiary amide instead of the carboxylate functions on the proton relaxometry, the thermodynamic stability and the kinetic inertness. Similarly to their results on DOTA derivatives, the presence of tertiary amides as pendant arms allows an increase of the stability of the complexes. However, the corresponding Mn(II)-complexes show quite low relaxivities, less than $2\ s^{-1}\cdot mM^{-1}$ at 37°C and 20 MHz, due to the absence of any innersphere water molecule. To increase the relaxivity, the denticity of the ligand has to be decreased and derivatives of PC2A (with 2 pendant arms) were developed. We can cite the

development of 3,6-PC2A and 3,9-PC2A depending on the position of the two acetate pendant arms (figure 2) [54]. The authors have found a better complex stability for the 3,9-PC2A complex compared to 3,6-PC2A, both complexes having one innersphere water molecule and being characterized by relaxivities similar to that of the clinically used Gd-DOTA (r_1^p = 2.72 and 2.91 mM^{-1} s^{-1} for the complexes 3,6-PC2A and 3,9-PC2A, respectively, at 25 °C and 0.47 T, table 1). Laurent *et al.* [55] have also developed three derivatives of 3,9-PC2A including an additional function grafted onto the pyridine ring to allow conjugation to a molecule of interest. Those three complexes are endowed with one innersphere water molecule and exhibit similar relaxivities than that of the 3,9-PC2A complex. Drahos *et al.* [56] have again decreased the denticity of the ligand by studying derivatives with one pendant arm (PC1A, figure 2). They have evaluated the influence of the nature of the coordinating group of this arm (acetate versus methylphosphonate group) on the thermodynamic stability, the kinetic inertness, the redox potential, and the ^1H and ^{17}O relaxation. They found that those mono-functionalized pyclens PC1A and PC1P give ternary hexacoordinate Mn^{2+} complexes accommodate with one water co-ligand, both of them being very labile and undergoing oxidation to the Mn^{3+} form, proving once again that the decrease of the denticity of the ligand is detrimental to the stability of the complexes.

Pyridine-based 15-membered macrocyclic ligands were also developed to complex manganese ions. Drahos *et al.* [57] developed Mn-15-pyN5 and Mn-15-pyN_3O_2 complexes (figure 2). They obtained a good thermodynamic and kinetic inertness, especially for Mn-15-pyN5, where the two additional nitrogen allows a higher thermodynamic stability, but this stability is nevertheless too low for *in vivo* applications. Moreover, their relaxivities were quite high thanks to the presence of two innersphere water molecules (table 1). Green *et al.* [58] also developed the same kind of complexes with an additional ortho-phenylene unit (Mn-15-pyN_3O_2-Ph, figure 2), but the stability was rather low so that it is unsuitable as MRI contrast agent. More recently, Drahos *et al.* [59] have added an additional acetate pendant arm on those pyridine-based 15 membered

ligands in order to increase the stability and the kinetic inertness, but also the solubility in water. The results show a decrease of the relaxivity compared to Mn-15-pyN5 and Mn-15-pyN_3O_2 complexes since the presence of the additional acetate pendant arm leads to a decrease of the number of innersphere water molecules from 2 to 1. The kinetic inertness is however a bit better but remains quite low for *in vivo* applications.

Recently, Mayilmurugan *et al.* [60] reported the design of new phenylenediamine based macrocyclic ligands to complex Mn(II) ions. Their results show good thermodynamic and kinetic inertness as well as interesting relaxivities, typical of complexes characterized by one water co-ligand, so that they could be promising for a future use as MRI contrast agents. We can also cite the study of Boschi *et al.* [61] who reported the development of a new class of Mn(II)-dithiocarbamates complexes. They obtained relaxivities similar to that of Gd-DOTA, but the stability tests have still to be done.

Globally, it can be evidenced that the thermodynamic stability and the kinetic inertness of the obtained Mn-complexes remains a major issue. Esteban-Gomez *et al.* [62] tried to analyze this stability using structural descriptors and evidenced some donor groups particularly suited to form stable chelates at physiological pH, such as 2-methylpyridine, secondary and tertiary acetamide or picolinate groups. A lot of efforts are however still to be done to obtain highly stable Mn-complexes with a good relaxivity, the most promising complexes appearing to be Mn-CDTA and its derivatives, Mn-PyC3A, Mn-PC2A and its derivatives, and Mn-1,4-DO2A and its derivatives.

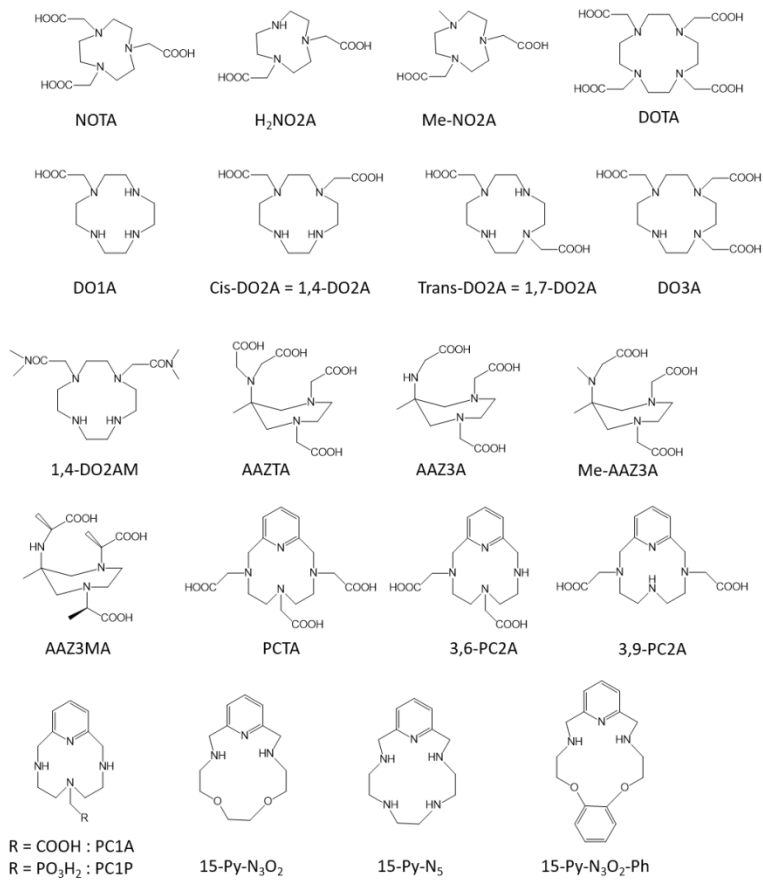

Figure 2: Structure of the macrocyclic ligands discussed in this work.

Liver Targeted Contrast Agents

The development of liver targeted MRI contrast agents has a double objective: first, it can allow the diagnosis of liver diseases such as tumors, and secondly an elimination through the liver instead of the kidneys could be safer for patients suffering from a kidney chronic disease. Mn-DPDP (figure 3) [21,22] was the first clinically used Mn-complex as liver targeted MRI contrast agent but it is no longer used because of its low relaxivity (2.8 $s^{-1} \cdot mM^{-1}$ at 20 MHz and 40°C) due to the lack of any innersphere water molecule, and toxicity issues due to the low

thermodynamic stability of the complex, which is releasing free Mn ions in vivo. Therefore, the development of those agents remains an important challenge.

Human organic anion transporting polypeptides (OATPs), expressed in functioning hepatocytes, can induce the cellular uptake of several amphiphilic organic molecules, such as bile salts, bilirubin, steroid hormones, thyroid hormones, and so on. Therefore, the development of amphiphilic Mn-complexes, bearing a lipophilic group on the chelate to mediate an uptake by the liver, is well-studied in the literature. It has moreover to be noted that a compromise has to be found between a sufficient lipophilicity to promote an avid hepatobiliary accumulation, and a rapid blood clearance to allow a fast diagnosis. Indeed, it has been shown previously that an increased lipophilicity can also promote binding to serum proteins, such as albumin, which will prolong the blood circulation time. The following Mn-complexes have shown interesting properties: Mn-EDTA-BTA [63], where the lipophilicity is provided by a benzothiazole aniline grafted on the EDTA coordination cage; complexes incorporating the well-known EOB (ethoxybenzyl) moiety, already used on Gd-complexes, on EDTA [64] (Mn-EDTA-EOB) , on CDTA [65] (Mn-CDTA-mA-EOB) or on PC2A [66] (Mn-EOB-PC2A); Mn-NOTA-NP [67], where a naphthalene group is grafted on NOTA; Mn-PyC3A-3-OBn [68], where a benzyloxy group is grafted at position 3 of the pyridine group of the chelator PyC3A; or Mn-BnO-TyEDTA [69-70], where the lipophilicity is also provided by a benzyloxy group introduced on the backbone of tyrosine-derived Mn-EDTA (figure 3). All those agents are endowed with a similar relaxivity comprised between 2.5 and 3.5 s^{-1} mM^{-1} at 1.5 T and 298 K (table 1) and undergo a partial renal and hepatobiliary excretion.

More specifically, a Mn-complex has recently been developed to image liver fibrogenesis. This pathology is accompanied by the upregulation of lysyl oxidase enzymes, which causes the apparition of aldehyde containing amino acid allysine (Lys^{Ald}) on the extracellular matrix proteins. A series of stable hydrazine-equipped manganese MRI probes able to bind to those modified proteins were thus developed, with promising results [71].

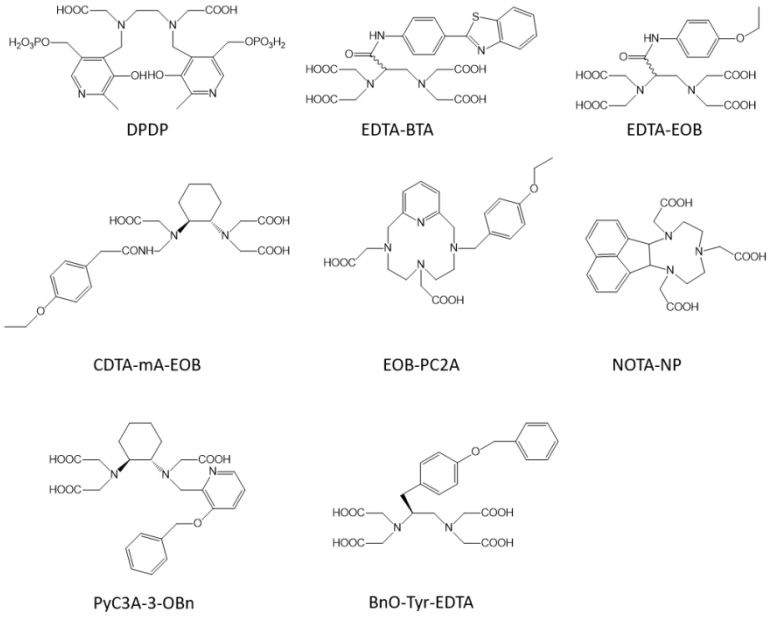

Figure 3: Structure of some ligands used to construct liver targeted contrast agents.

Blood Pool Agents

Blood pool agents are characterized by a long vascular circulation time, so that they can be used for vascular imaging. MR hardware allows now to record high quality vascular images with extracellular agents few seconds after the injection, so that the development of blood pool agents appears less important [32]. Nevertheless, they could still be interesting for some specific applications, such as highlighting microvascularization in tumors.

Targeting HSA (human serum albumin), one of the most abundant protein in the blood plasma, is the most common method in the literature. HSA has two binding sites in its tridimensional structure which are known to bind organic molecules with hydrophobic moieties. Different strategies can thus be evidenced to target HSA: (i) the grafting of different hydrophobic moieties on common used chelates. We can cite the

grafting on EDTA of one or two benzyloxymethyl (BOM) groups [72], of the same moiety than that used in MS-325 (Mn-LCyPh$_2$) [73], or of deoxycholic acid [74]; the grafting of a biphenyl substituent on the ligand PC2A [75]; the grafting of benzyl groups on the 1,4-DO2AM platform (1,4-BzDO2AM, 1,4-DO2AM-Bz and DO2AMGly) [76,77]; or the grafting on NOTA of the truncated Evans blue dye [78] (figure 4) (ii) the chelate itself can have hydrophobic moieties able to promote a binding to HSA. It is the case for Mn-PyC3A [32-34] (figure 4); for the Mn-complex developed by Stasiuk *et al.* [40]; for ligands developed by Platas-Iglesias *et al.* [79] containing pentadentate 6,6'-((methylazanediyl)bis(methylene)dipicolinic acid binding units able to form mono- (H_2dpama), di- (mX(H_2dpama)$_2$), and trinuclear (mX(H_2dpama)$_3$) complexes with Mn^{2+} ions (figure 4); or for aza-semi-crown pentadentate ligands rigidified by pyridine and piperidine rings developed by Ai *et al.* [80] For all those complexes, a huge increase of the relaxivity is observed in the presence of HSA due to the formation of a non-covalent adduct (table 1).

Another strategy consists in the development of amphiphilic paramagnetic complexes, able to form micelles endowed with a high plasmatic half-life and a high relaxivity. Tei *et al.* [81,82] synthesized six original amphiphilic ligands based on EDTA or on DO2A, grafted with aliphatic chains. A strong self-association in micelles was observed, resulting in an enhanced relaxivity. Furthermore, micelles were able to interact with HSA, increasing even more the relaxivity. In another study, PEGylated amphiphilic polymeric Mn-complexes were developed and showed an enhanced relaxivity as well as an excellent and relatively long time-window vascular enhancement effect [83,84].

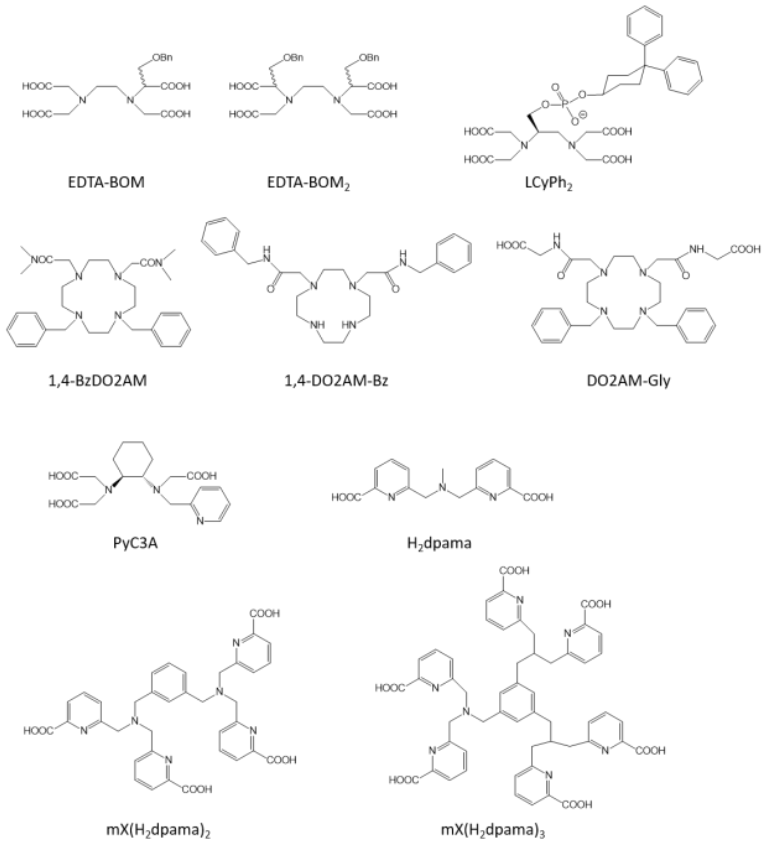

Figure 4: Structures of some of the ligand used for the design of the blood pool agents described in this work.

Responsive Contrast Agents

Responsive contrast agents, also called smart or intelligent CAs, are able to report changes of a physiologically relevant parameter, such as pH, redox state, levels of some endogenous ions (Zn^{2+}, Ca^{2+} or Cu^{2+}), etc.

Mapping of tissue pH could allow the diagnosis of tumors at an early stage since their enhanced glucose metabolism induce a decrease of the extracellular pH (Warburg effect) [85]. pH responsive contrast agents will be able to evidence this pH decrease by a change in their relaxivity, induced by a change in the number of coordinated innersphere water molecules. A first

example is the Mn-PC2A-EA [86] with an ethylamine pendant arm (figure 5). At acidic pH (between 3.7 and 5.8), the protonation of the amine function allows the presence of one innersphere water molecule, with a relaxivity of 3.5 s^{-1} mM^{-1} at 0.47 T and 25°C, but when the pH increases, the deprotonation of the amine function allows its coordination to the metal, inducing the loss of the innersphere water molecule and hence a decrease of the relaxivity to 2.1 s^{-1} mM^{-1} (table 1). Other studies have used the interesting protonation transition of sulfonamides groups around the physiological pH to construct pH responsive contrast agents. Platas-Iglesias *et al.* [42] developed several complexes characterized by a transition from one innersphere water molecule at basic pH to two innersphere water moleules at acidic pH, with a relaxivity changing from 3.8 s^{-1} mM^{-1} at pH 9 (10 MHz, 25°C) to 8.9 s^{-1} mM^{-1} at pH 4. In a more recent study involving a sulfonamide group grafted on a triazacyclononane macrocycle, Liang *et al.* [87] observed a change in relaxivity from 0.9 s^{-1} mM^{-1} at pH 7-9.5 (20 MHz, 25°C), characteristic of a q=0 complex, to 3.0 s^{-1} mM^{-1} at pH 7-4.5, typical of the presence of one innersphere water molecule.

A modification of the redox status of tissues is a well-known feature of different diseases such as cancers, ischemia or chronic inflammation. Being able to detect changes in redox activity *in vivo* could thus be very important in the diagnosis of those pathologies. In that aim, using the couple Mn(II)/Mn(III) ions can be an elegant method to monitor redox imbalance. Indeed, Mn(II)-complexes are generally characterized by higher relaxivities than their Mn(III) equivalents, as explained earlier. Caravan *et al.* [88-90] have largely exploited this way by developing several generations of complexes based on the EDTA core modified with one or several hydroxybenzyl moieties (HBET, HBED, JED, figure 5), able to form stable complexes with both Mn(II) and Mn(III) ions. The more recent system based on the JED ligand allows to observe a 9-fold enhancement of the relaxivity when Mn(III) is reduced to Mn(II) (table 1).

The detection of oxidative stress is also a major challenge since it is linked to tissue damage in many diseases (Alzheimer, Parkinson, atherosclerosis, …). Being accompanied by the production of reactive oxidative species (ROS), Mn-complexes

able to directly detect ROS have been developed [91,92]. Two generations were elaborated: the first one is based on an original ligand (N-(2-hydroxy-5-methylbenzyl)-N,N′,N′-tris(2-pyridinylmethyl)-1,2-ethane-diamine, Hptp1, figure 5) able to form a stable complex with Mn(II) ions. Upon reaction with H_2O_2, the complex couple to itself to form a dimer, with a resulting decrease of the relaxivity. This strategy has however the disadvantage that the production of ROS would be detected by a decrease of the contrast (negative contrast) [91]. A second generation was thus developed where an oxidizable quinol group is grafted on the same type of ligand. This allows to observe an increase of the relaxivity upon the presence of H_2O_2 (table 1) [92].

ROS being produced notably by Myeloperoxidase (MPO), a heme protein, another strategy consists in developing contrast agents of which the relaxivity is modified when this enzyme is overexpressed. This is the case for the complex Mn-Tyr-EDTA (figure 5), where a tyrosine derivative is grafted on EDTA, and which demonstrates a peroxidase activity-dependent relaxivity by forming oligomers in the presence of the enzyme, inducing an increase of the relaxivity (table 1) [93].

Another example of responsive Mn-based contrast agent was developed by Tircso *et al.* [94]. They synthesized a 3,9-PC2A derivative, grafted with a di-(2-picolyl)amine (DPA) moiety as an active arm (figure 5), able to selectively bind Zn^{2+} ions in the co-presence of human serum albumin, with an increased relaxivity (table 1). This complex is moreover characterized by a good thermodynamic stability (pMn = 8.79) and a high kinetic inertness towards zinc transmetallation ($t_{1/2}$ at pH 6.0 = 64.5h).

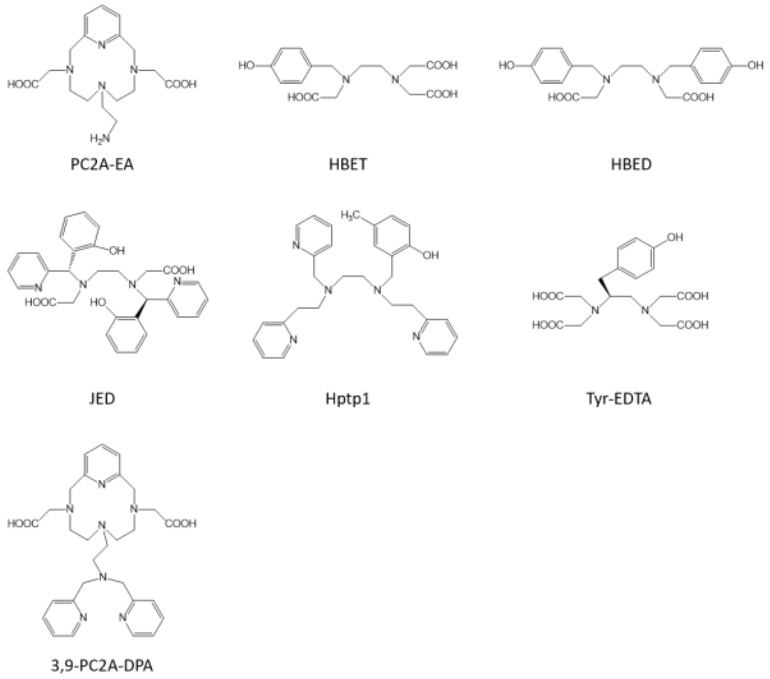

Figure 5: Structures of some of the ligands used to obtain responsive contrast agents.

Multimodal Contrast Agents

Multimodal contrast agents are designed to be used in different imaging techniques. One bimodality well developed in the clinical field is the combination of MRI with PET (positron emission tomography) [95], since it allows to couple the high resolution of MRI with the high sensitivity of PET. As MRI images can be recorded without the use of any contrast agents, dual PET/MRI can be performed with single PET probes. Nevertheless, the development of dual MRI/PET probes is important because MRI images will also benefit from a contrast enhancement, which, if we refer to all the studies described before, could be tissue-specific or biomarker-responsive. The positron-emitting ^{52}Mn having interesting decay properties ($t_{1/2}$ = 5.6 d) for PET imaging, dual probes able to complex radioactive ^{52}Mn and cold ^{55}Mn are thus promising. This allows to overcome the major problem of combining both techniques in the same

probe, i.e. the big sensitivity difference between both techniques which necessitate millimolar concentrations for MRI and nanomolar concentrations for PET. Moreover, it also guarantees that both reporter molecules are chemically identical and hence endowed with a similar biodistribution. Neumaier *et al.* [96] have described the development of such a probe, by grafting on the CDTA chelate different functional groups. They obtained Mn-complexes with good thermodynamic and kinetic stabilities, as well as interesting relaxivities. Another group has developed dual PET/MRI probes based on a 3,9-PC2A derivative, where one of the amine nitrogen was replaced by an etheric oxygen atom, which decreases the basicity of the ligand, without affecting its stability when complexed with Mn(II) ions [97].

Another well-developed bimodality is the combination between MRI, characterized by a high resolution, and optical imaging, endowed with a good sensibility. The reporter probes for optical imaging are fluorescent molecules, emitting light in the near-infrared (NIR) to limit the absorption by the tissues. Those fluorescent molecules could be grafted on Mn-based contrast agents, and it has been exploited recently by Edwards *et al.* who grafted hydrophobic functional groups, as chromophores, on EDTA bisamides [98]. Another study of Zhang *et al.* [99] describes two kinds of terpyridine–Mn(II) complexes (FD–Mn–O_2NO and FD–Mn–FD, figure 6**)** possessing seven and six coordination modes, respectively, as dual probes for multi-photon fluorescence imaging (MP-FI) and MRI. The second complex FD-Mn-FD is the most promising one, with interesting optical properties (excitation wavelength at 1450 nm (NIR-II)) and relaxometric properties (r_1 = 2.6 s^{-1} mM^{-1} at 20 MHz and 25°C). Moreover, this complex could also act as a therapeutic agent for the treatment of cancer by photodynamic therapy (PDT). This technique uses a photosensitizer, which, upon activation by light, can kill cancer cells. In that study, FD–Mn–FD generates endogenous $^1O_2$ under irradiation by 808 nm light, thereby enhancing the PDT effect in vitro and in vivo.

Table 1: Relaxometric properties and application area of the molecular Mn-complexes discussed in this work.

	q	r_1 in water or buffer (s^{-1} mM^{-1})	r_1 in the presence of HSA (s^{-1} mM^{-1})	Application area	Tested *in vitro* and/or *in vivo*
Mn-EDTA	1	2.9 (0.47T, 35°C, [27])		extracellular	no
Mn-CDTA	1	3.0 (0.47T, 40 °C, [30])		extracellular	no
Mn-PyC3A	1	2.1 (1.4T, 37°C, [31])	3.5 (1.4T, 37°C, [31])	extracellular/ blood pool	yes [33,34]
Mn-DPAA	1	2.7 (0.47T, 37°C, [35])		extracellular	no
Mn-DPAMeA	2	5.1 (0.47T, 37°C, [35])		extracellular	no
Mn-DPAPhA	2	4.2 (0.47T, 37°C, [35])		extracellular	no
Mn-PAADA	2	3.3 (0.47T, 37°C, [36])		extracellular	no
Mn-AMPTA	1	2.6 (0.47T, 37°C, [37])		extracellular	no
Mn-AMPDA-HB	1	2.7 (0.47T, 37°C, [37])		extracellular	no
Mn-MeNO2A	1	2.2 (0.47T, 37°C, [46])		extracellular	no
Mn-DO3A	0	1.3 (0.47T, 37°C, [49])		extracellular	no
Mn-1,7-DO2A	0	1.3 (0.47T, 37°C, [49])		extracellular	no
Mn-1,4-DO2A	1	1.7 (0.47T, 37°C, [49])		extracellular	no
Mn-1,4-DO2AM	1	2.0 (0.47T, 37°C, [51])		extracellular	no
Mn-AAZTA	0	1.6 (0.47T, 25°C, [53])		extracellular	no
Mn-AAZ3A	1	2.5 (0.47T, 25°C, [53])		extracellular	no
Mn-MeAAZ3A	1	2.0 (0.47T, 25°C, [53])		extracellular	no
Mn-AAZ3MA	1	1.9 (0.47T, 25°C, [53])		extracellular	no
Mn-3,6-PC2A	1	2.7 (0.47T, 25°C, [54])		extracellular	no
Mn-3,9-PC2A	1	2.9 (0.47T, 25°C, [54])		extracellular	no
Mn-15-pyN_5	2	3.1 (0.47T, 37°C, [57])		extracellular	no
Mn-15-pyN_3O_2	2	3.6 (0.47T, 37°C, [57])		extracellular	no
Mn-EDTA-BTA	1	3.5 (1.5T, 24°C, [64])	15.1 (1.5T, 24°C, [64])	liver	yes [63]
Mn-EDTA-EOB	1	2.3 (1.5T, 24°C, [64])	6.3 (1.5T, 24°C, [64])	liver	yes [64]
Mn-EOB-PC2A	1	2.8 (1.5T, 25°C, [66])	5.9 (1.5T, 25°C, [66])	liver	yes [66]
Mn-NOTA-NP	1	3.6 (3T, 25°C, [67])	9.0 (3T, 25°C, [67])	liver	yes [67]
Mn-PyC3A-3-Obn	1	2.6 (1.4T, 37°C, [68])	9.0 (1.4T, 37°C, [68])	liver	yes [68]
Mn-BnO-TyEDTA	1	4.3 (0.47T, 32°C, [69])	15.8 (0.47T, 32°C, [69])	liver	yes [69,70]
Mn-EDTA-BOM	1	3.6 (0.47T, 25°C, [72])	55.3 (0.47T, 25°C, [72])	blood pool	no

Mn-LCyPh2	1	5.8 (0.47T, 37°C, [73])	48.0 (0.47T, 37°C, [73])	blood pool	yes [73]
Mn-1,4-BzDO2AM	1	3.8 (0.47T, 25°C, [76])	18.5 (0.47T, 25°C, [76])	blood pool	no
Mn-1,4-DO2AM-Bz	1	3.5 (0.47T, 25°C, [76])	27.4 (0.47T, 25°C, [76])	blood pool	no
Mn-DO2AM-Gly	1	4.5 (1T, 25°C, [77])	14.0 (1T, 25°C, [77])	blood pool	yes [77]
Mn-dpama	2	4.2 (0.47T, 37°C, [79])	12.2 (0.47T, 37°C, [79])	blood pool	no
mX(Mn-dpama)$_2$	2	6.1 (0.47T, 37°C, [79])	39.0 (0.47T, 37°C, [79])	blood pool	no
mX(Mn-dpama)$_3$	2	8.3 (0.47T, 37°C, [79])	45.2 (0.47T, 37°C, [79])	blood pool	no
Mn-PC2A-EA	1	3.5/2.1 (0.47T, 25°C, [86])		pH responsive	no
$Mn^{II/III}$-HBET	1	1.0/2.8 (1.4T, 37°C, [88])		redox responsive	no
$Mn^{II/III}$-JED	1	0.5/3.3 (1.4T, 37°C, [90])		redox responsive	no
Mn-Hptp1	1 / 2	4.7/5.3 (3T, 25°C, [92])		redox responsive	no
Mn-Tyr-EDTA	1	3.3/8.5 (0.47T, 32°C, [93])	8.0 (0.47T, 32°C, [93])	redox responsive	yes [93]
Mn-3,9-PC2A-DPA	1	3.2 (1.4T, 37°C, [94])	12.1 (1.4T, 37°C, [94])	Zn responsive	yes [94]

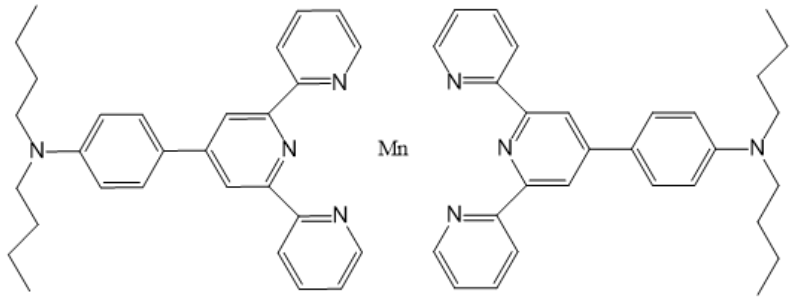

Figure 6: Structure of the theranostic agent FD-Mn-FD.

In vitro/in vivo Studies and Toxicity Issues

As shown in table 1, only a few Mn-complexes were tested *in vitro* and/or *in vivo*. Surprisingly, most of those complexes are endowed with an increased lipophilicity, allowing their use as liver targeting contrast agents or blood pool agents. Biodistribution studies by MRI and ICP show a dual renal and hepatobiliary elimination for all those agents, which is explained by their enhanced lipophilicity compared to small extracellular agents like Gd-DOTA. Mn-PyC3A was also tested in a rat model of renal impairment, and the *in vivo* studies indicate in that case an increased hepatobiliary elimination [34]. Mn levels had moreover returned to baseline within 24 h after injection for all those complexes.

Their efficacy as MRI contrast agents was also tested. Liver targeted contrast agents were systematically injected in a murine liver tumor model to evaluate their ability to differentiate normal liver and tumor tissue. MRI images show for most of the complexes a hypointense signal in tumor tissues compared to normal liver tissues after injection of the Mn-complex. This can be explained by the transport mechanism of the Mn-complexes to the liver: they can enter normal hepatocytes through organic anion-transporting polypeptide transporters (OATPs), which are considerably reduced in tumor tissues. The study of Zhu et al. [69] has particularly evidenced the importance of OATPs in the hepatic uptake of Mn-complexes by performing images in the presence of an OATP inhibitor, as well as cell uptake studies on OATP-transfected and non-transfected cell lines. Nevertheless,

the study on Mn-NOTA-NP [67] contradicts the above results since a hyperintense signal is observed in tumor tissues compared to the normal liver. The authors explain this result by a decreased MRP2 expression in tumor cells, whereas OATPs expression is maintained. As the role of MRP2 is to mediate the secretion of the Mn-complex from the tumor cells to the lumen, its decreased expression induces an accumulation of the Mn-complex in the cytoplasm of tumor cells, which explains the observed hyperintense signal. Thus, it evidences the need of more thorough investigations in the future. A few blood pool agents have also been studied in vivo to evaluate their efficacy. Mn-LCyPh$_2$ was injected into white rabbits at doses of 30 µmol/kg and 10 µmol/kg, and good vascular images could be obtained for both doses. The authors were also able to distinguish injured from normal vessels [73]. The study on Mn-DO2AM-Gly was more focusing on the ability of the Mn-complex to accumulate in a highly vascularized tumor model, and interesting results were obtained on subcutaneous breast tumor lesions, where a strong contrast enhancement was obtained [77]. The redox responsivity of Mn-Tyr-EDTA was also evaluated in vivo on a murine model with monosodium urate crystal-induced acute gouty arthritis. The contrast enhancement in the inflammation site was higher than that obtained with Gd-DTPA, used as control.

Even if the above studies are encouraging, very few data exist about the possible toxicity of all those agents. Some of the abovementioned studies present cell viability assays [63,64,67,69,77] to evaluate the toxicity of the Mn-complexes. The results showed a negligible cytotoxicity towards various cell lines in the concentration range needed for MRI. Nevertheless, it is not sufficient at all to attest of a safe use of those complexes *in vivo*. Indeed, as for Gd-complexes, the release of free Mn^{2+} ions *in vivo* could be responsible of pathological disorders for patients, such as Manganism, a disease with symptoms close to these of the Parkinson's disease. It is thus crucial to verify that the Mn-complexes remain intact when they are injected *in vivo*, which is nearly never the case. The study of Caravan *et al.* [73] on Mn-LCyPh$_2$ mentions that the complex should remain intact since any acute cardiac toxicity was evidenced during their

study, and free Mn^{2+} ions are known to be very toxic for the heart. This is nevertheless an indirect proof, so that more thorough studies, such as those performed on gadolinium complexes when concerns about NSF and gadolinium retention in the brain start to appear, are needed to attest the safety of all those Mn-complexes. The scientists must take advantage of the knowledge acquired about gadolinium complexes to avoid repeating the same mistakes and develop newer and safer MRI contrast agents.

Nanoparticular Contrast Agents

Nanoparticles Incorporating Mn-Complexes

The aforementioned Mn-complexes are globally characterized by limited relaxivities and an elegant manner to increase their efficacy is the increase of their rotational correlation time τ_R, even by an increase of their molecular weight or by their incorporation in nanosystems. This has been largely exploited in the literature.

As described previously [81-84], amphiphilic Mn-complexes can be assembled in lipidic nanoobjects, such as micelles or liposomes, with considerable relaxivities. For example, Ai *et al.* [84] have co-assembled amphiphilic Mn-chelates (C18-PhDTA-Mn) with amphiphilic PEG-C18 polymers to obtain mixed micelles of different hydrodynamic sizes and relaxivities up to 13 s^{-1} mM^{-1} at 1.5T and 25°C.

Dendrimeric nanosystems are another well-exploited method to increase the rotational correlation time of Mn-complexes. Lu *et al.* [100-101] describe the grafting of Mn(II)-DOTA monoamides on lysine dendrimers with a silsesquioxane core. Different generations (G2, G3 and G4) of dendrimers were synthesized, with a decrease of the per ion relaxivity when the generation of the carriers increases. This can be explained by the lack of any innersphere water molecule on the Mn-DOTA complexes, as explained previously. The relaxivity comes thus only from a secondary solvation sphere due to hydrogen bonding between water and Mn-complexes, and from a less organized outer solvation sphere. As the dendrimers generation is

increasing, the probability of hydrogen bonding is also increasing, which could increase the residence time of water molecules in the secondary sphere and have a detrimental effect on the relaxivity. Moreover, DOTA chelates could be buried in the higher generations, and less accessible to solvation. The authors tried also to replace DOTA by NOTA, and they obtained a better relaxivity thanks to the presence of one innersphere water molecule. More recently, Gao *et al.* [102,103] describe three generations of DOTA-branched organic frameworks constructed by uniting DOTA building blocks. They carefully characterized the kinetic inertness of their systems and obtained an inertness 69-fold higher than that of Magnevist. This could be explained by three factors: (i) the chelates in the macromolecular structure are considerably "squeezed", which hinders the release of Mn^{2+}; (ii) the positively charged core of the nanosystems repels protons and other positively charged ions, increasing the kinetic inertness; (iii) the metal ions released from the dendrimers could be recaptured by the numerous chelating groups, increasing the time needed to completely release Mn^{2+}. We can also cite the work of Caravan *et al.* [28], already described in a previous section, who has grafted six tyrosine-derived EDTA moieties on a cyclotriphosphazene core.

The incorporation of Mn-complexes inside nanosystems is also an interesting path to explore. Botta *et al.* [104] have incorporated Mn-CDTA bisamides complexes in nanogels based on a chitosan matrix. The Mn-complexes are covalently grafted on chitosan and act as contrast media and as cross-linking agents. They obtained relaxivities seven times higher than that of small Mn-complexes, thanks to the restricted mobility of the complex combined with a fast exchange of the innersphere water molecule. The stability at physiological pH is moreover very good. Another study explores the non-covalent encapsulation of a hexadentate pyridine-picolinate Mn-complex within a porous silica nanosphere. The entrapped complex exhibits a relaxivity at 25°C and 1.41 T 2.9 times higher than that of the unentrapped complex. The kinetic inertness towards Zn^{2+} ions and physiologically relevant anions (bicarbonates, biphosphonates, citrate) is also very good [105]. Axelsson *et al.* [106,107] develop an organophosphosilane hydrogel with strongly chelated

manganese (II) ions and a covalently attached PEG surface layer. This nanosystem has a globular shape, an average hydrodynamic diameter of 5 nm and a relaxivity of 30 s^{-1} mM^{-1} at 1.41 T and 25°C. It is currently evaluated in a Phase IIa clinical trial as an open-label, proof-of-concept study evaluating its safety and MRI-enhancing properties in adult female patients with suspected endometrial lesions. (NCT05664828).

Mn-complexes can also be grafted at the surface of inorganic nanoparticles, such as silica nanoparticles. Mn-DTPA derivatives were grafted at the surface of mesoporous silica nanoparticles, with a good relxivity of 7.18 s^{-1} mM^{-1} at 25°C and 1 T [108]. Nevertheless, even if the porous structure provides an easy access for water protons, the enhanced relaxivity is limited by the fact that there is no innersphere water molecule on the DTPA chelates. In a more recent study, Mn(II)-CDTA derivatives were grafted onto silica nanoparticles [109]. The obtained relaxivity at 1T and 25°C is higher (around 12 s^{-1} mM^{-1}) than for the previous study thanks to the presence of one innersphere molecule.

Mn-based Organic/Inorganic Nanoparticles

Mn ions can also be incorporated in the structure of the nanoparticles and a lot of examples are available in the literature. Nanoparticles have indeed a lot of advantages such as the tunability of their size and shape, a high surface to volume ratio, and the possibility to easily functionalize them to obtain targeted, multimodal or theranostics agents [110,111]. Even if a comprehensive review of those systems extends beyond the scope of this viewpoint, the most relevant examples are cited below.

Manganese oxide nanoparticles (MONs), such as MnO, MnO_2, and Mn_3O_4 are well studied as T_1 MRI contrast agents [112-114], and more particularly MnO nanoparticles as the oxidation state of Mn is +2, assuring five unpaired electrons, and hence a better efficacy to increase water T_1 relaxation rate. The efficacy coming from the Mn ions at the surface, two crucial factors to have a high relaxivity can be highlighted: (i) the size of the nanoparticles, which as to be as small as possible to enhance the

surface to volume ratio, and (ii) the coating used to stabilize the nanoparticles, which has to be as hydrophilic as possible to assure a good penetration of water. Moreover, MnO nanoparticles can be retained by the reticuloendothelial system (RES) and subsequently accumulating in liver and spleen, leading to Mn^{2+}-induced toxic effects. The coating has thus to be cleverly chosen in order to limit the capture by the RES. Different coatings have been tried in the literature such as polymer functionalization [115-117] (and particularly polyethylene glycol (PEG) coating), silica coating [118] or phospholipid modification [119]. Even if all those nanosystems can accumulate passively in tumors by the EPR effect, some researchers also added specific targeting ligands (such as aptamers or cRGD peptide) to increase the uptake by the tumor over a long period of time [115,116,120]. T_1-T_2 dual mode contrast agents, obtained by combining MnO (as T_1 agent) and Fe_3O_4 (as T_2 agent), have also been extensively studied [121,122]. The bimodality can also come from another imaging technique, as optical imaging (OI), which is a more sensitive imaging technique than MRI, as explained in a previous section. MnO nanoparticles can easily be functionalized by near-infrared dyes, such as Cy5.5, as contrast agent for OI [123,124].

Besides the development of manganese oxide nanoparticles, Mn ions have also been incorporated in other types of inorganic nanoparticles. We can cite the incorporation of Mn ions in cyano-bridged coordination networks, such as Prussian blue nanoparticles [125], the grafting of manganese ions on the surface of nanodiamonds [126,127], the encapsulation of Mn^{2+} ions in sealed carbonized shells [128], or the development of carbon dots doped with manganese [129,130]. This last system has the advantage of being detectable also in optical imaging since carbon nanodots are luminescent. All those described systems are characterized by higher relaxivities than the small Mn-complexes described in section 2 and are thus good candidates as T_1 MRI contrast agents. Dual T_1/T_2 agents are also developed. Zhang *et al.* [131] designed ferroferric oxide coated by Mn-doped silica as an intelligent MRI nanoswitch. Under normal tissue conditions, the nanostructure is very stable, so that the r_1 and r_2 relaxivities are very low, but the slightly acidic pH

of tumors is responsible of the nanostructure collapse, releasing the Mn^{2+} ions, which are separated from the Fe_3O_4 magnetic core, with a resulting increase of the relaxivities r_1 and r_2.

Organic nanoparticles are also well exploited in the literature to incorporate manganese ions. More particularly, metal organic frameworks (MOFs), where a small ligand and a metal center are alternatively linked together to form a porous structure with a defined shape, have attracted much attention. For example, Aoki *et al.* [132] developed Mn-MOF-74, where the ligand dihydroxyterephthalate (DHTP) self-assemble with Mn^{2+} ions to form a honeycomb-like structure with a diameter of 1.0 nm. They obtained an interesting relaxivity of about 10 s^{-1} mM^{-1} at 1.0 T and 23°C. Zhao *et al.* [133] developed Mn(II)-chelated ionic covalent organic framework (iCOF) and also obtained an interesting relaxivity (8 s^{-1} mM^{-1} at 3.0 T and 25°C). Natural organic particles can also be used, such as proteins, and this has notably been exploited recently by Colombo *et al.* [134], who have loaded Mn ions in H-ferritin, a recombinant variant of human apoferritin consisting of 24 self-assembled heavy-chains subunits. Two formulations were prepared, at room temperature and at 65°C, with a very low relaxivity for the latter compared to the formulation at room temperature. This was explained by the oxidation of the Mn ions to Mn^{3+}, Mn^{4+} and Mn^{7+} in the formulation obtained at high temperature.

In vitro/in vivo Tests and Toxicity Issues

Nanoparticles Incorporating Mn-Complexes

Most of the presented systems were studied *in vivo* to evaluate their efficacy as MRI contrast agents. Overall, they are eliminated through the kidneys or the liver according to their size, and they are also able to accumulate in tumors and/or lymph nodes due to the enhanced permeability and retention effect (EPR). This effect is based on the abnormalities that appear in the tumor microenvironment. Indeed, tumors exhibit poor lymphatic drainage and vessels with a higher permeability than healthy vessels. These two points allow an accumulation of the nanostructures in the tumor site, which could favor tumor diagnosis.

Nevertheless, as already mentioned in the previous section concerning the small Mn-complexes, very few toxicity data are available. Again, some studies present encouraging cytotoxic studies on various cell lines [84,103,104,108], which do not show any acute toxic effect. We can also cite the study of Ai *et al.* [83], who have measured key serum biochemical indicators of liver function and kidney function and found a normal range for all of them. Gao *et al.* [103] also evidenced the absence of tissue injury or inflammation in any of the major organs 2 days after the injection of their dendrimeric nanosystems. All of those indicators are very encouraging but more systematic studies of the toxicity are still missing.

Mn-based Organic/Inorganic Nanoparticles

Those nanoparticles were almost all tested *in vitro* and *in vivo*, and exhibit overall interesting properties as T_1 MRI agents. Cytotoxic studies on various cell lines indicate a globally good cell viability for most of the tested systems, and most of the *in vivo* studies do not report any pathological abnormalities through hematoxylin and eosin (H&E) staining of the major organs (heart, kidney, liver, lung and spleen). This is thus encouraging and suggest that most of the cited nanosystems have a low cytotoxicity and a good biocompatibility. Nevertheless, as already mentioned for the previous systems, more systematic studies of the toxicity of those nanoparticles are needed. At the moment, all the studies are focused on the performance of the systems as MRI contrast agents, but a translation to the clinic will necessitate the establishment of a transparent cytotoxicity pattern.

Theranostic Agents

Mn-based theranostic agents, combining an MRI contrast agent based on manganese and a therapeutic tool, are more and more developed in the literature, especially in the field of cancer diagnosis and treatment. Only few molecular examples are described. Additionally to the study of Zhang *et al.* [99] (see previous section), a salinomycin-based paramagnetic complex of manganese was synthesized. To overcome its water insolubility, it was loaded into empty bacterial ghosts (BGs) cells as transporters. Its relaxivity is similar to the one reported for small

Mn-complexes, and it was able to induce perturbations in the cell cycle of colorectal and breast human cancer cell lines [135]. Nevertheless, most of the researches concern nanoparticular agents since it is quite easy to modify their surface to incorporate several functional moieties [136-138]. Even if a detailed description of all the developed systems is beyond the scope of this review, we can cite some recent relevant examples.
Nanoparticular agents can be divided in two categories:

i. nanoparticles incorporating a drug (such as doxorubicin, cisplatin, paclitaxel, or docetaxel) able to kill cancer cells. Different studies are available in the literature. For example, the development of polymeric micelles or vesicles (polymersomes) incorporating doxorubicin is described. Alibolandi *et al.* [139] described the development of polymersomes based on a amphiphilic diblock copolymer of poly(ε-caprolactone)-block-poly(glyceryl methacrylate) encapsulating doxorubicin in the hydrophilic core of the vesicles and a hydrophobic Mn-complex based on phenanthroline in the bilayer membrane. An aptamer was moreover added on the surface to increase the specificity of the nanosystem for colorectal cancer cells. Another study has designed a nanosystem based on a hydrophobic core made of doxorubicin complexed with Mn^{2+} ions, stabilized by an outer layer composed of a self-assemblied amphiphilic block copolymer distearyl phosphatidylethanolamine-polyethylene glycol (DPSE-mPEG2000) [140]. Both systems show good therapeutic and MRI abilities to treat and monitor tumors. Inorganic nanoparticles are also developed. As an example, the design of pH-responsive Mn-ZnO nanoparticles was recently described. The nanoparticles are coated with polyacrylic acid, and decorated with folic acid to target tumor cells. Doxorubicin is loaded in the system through electrostatic interactions with polyacrylic acid and can be released from the nanocomposite at slightly acidic pH [141].
ii. nanoparticles uncluding other therapeutic tools, such as photodynamic therapy (PDT), or photo-thermal therapy (PTT), which are both light-excited treatment prototypes. PDT induces the production of reactive oxygen species (ROS) through light activation of photosensitizers, whereas PTT uses photothermal conversion agents to generate heat

and kill cancer cells. The design of Mn-doped magnetosomes was reported recently [142]. They are naturally produced through the biomineralization of magnetotactic bacteria by doping manganese into the iron oxide crystals. The further functionalization of the surface with cRGD peptides allows an accumulation in tumors. This agent can act as a dual T_1/T_2 MRI agent, and has also a good optical absorbance in the NIR region, leading to a high photothermal capability. Another study is using rod-like cellulose nanocrystals coated with crosslinked polydopamine as photothermal agents, and Mn^{2+} ions were embedded into the crosslinked polymeric coating as MRI contrast agents. Interesting relaxivity and photothermal conversion efficiency of 38 s^{-1} mM^{-1} (at 3T and 25°C) and 44% (after irradiation at 808 nm with an output power of 2 $W.cm^{-2}$ during 12 min) were respectively obtained [143]. Smart systems, avoiding side effects in normal tissues, are also more and more developed. Zhao *et al*. [144] designed a switchable nanosystem which can act as a ROS scavenger in normal tissues, and as a ROS generator in tumor microenvironment during PDT. It is based on a Mn_3O_4 nanozyme coated with 1,2-distearoyl-sn-glycero-3-phosphoethanolamine-N-[amino(polyethylene glycol)-2000] (DSPE-PEG_{2000} amine) to insure the solubility in water, and loaded with pyropheophorbide, as PDT agent. This nanosystem is able to down-regulate ROS with dampened cytokine wave in normal tissues after PDT, whereas in the tumor microenvironment, glutathione (GSH), which is known to be overexpressed in cancer cells, will degrade the nanosystem, increasing the production of $^1O_2$. The oxidative stress of the tumor tissue will be moreover increased through the liberation of Mn ions during the degradation. They are indeed able to produce cytotoxic hydroxyl radicals ($^\bullet$OH) via a Fenton reaction with H_2O_2. Additionally, the released Mn ions show a strong T_1 MRI contrast.

iii. Chemodynamic therapy (CDT) is also more and more developed. It is based on the principle described above, i.e. the production of cytotoxic hydroxyl radicals ($^\bullet$OH) via a Fenton reaction with H_2O_2. Mn-based nanoparticles are particularly useful in that case, especially MnO_2

nanoparticles, since Mn^{4+} ions can be reduced to Mn^{2+} by GSH. The produced Mn^{2+} ions can then enhance T_1-MRI, but also react with H_2O_2 by a Fenton reaction to produce hydroxyl radicals ($^{\bullet}OH$). Those nanoparticles are thus good candidates as theranostic agents and this was well exploited in the literature, where a lot of different morphologies are described such as core-shell, hollow-spherical, Janus, nanoflower, honeycomb, or nanosheet structures [136]. For all these hybrid nanoparticles, the MnO_2 nanoparticles are incorporated in other materials or their surface is modified to assure their stability and to optimize their efficacy. Purely inorganic materials are described, such as graphitic carbon nitride-manganese oxide nanoflowers (g-C_3N_4/MnO_2) [145], but hybrid inorganic/organic nanosystems are also very well-developed. For example, Wang *et al.* [146] employed poly(lactic-co-glycolic acid) (PLGA) nanoparticle as a template to synthesize hollow MnO_2. In the acidic tumor microenvironment, the fast degradation of hollow MnO_2 nanoparticles induces the liberation of Mn^{2+} ions, catalyzing the transformation of H_2O_2 to $^{\bullet}OH$ for CDT. In this study, bufalin was also incorporated in the nanosystem as a chemotherapeutic drug, released during the degradation of the hollow MnO_2 nanoparticles.

A lot of studies tried also to combine several therapeutic tools in the same nanoobject (combination therapy) to increase the chances to kill the tumor cells. The combination between PTT and/or PDT with CDT, or with the use of a chemotherapeutic drug, or the combination between CDT and the use of a chemotherapeutic drug, or in some studies the combination between all those techniques, are often reported. As examples, we can cite the combination of CDT with the use of paclitaxel as chemotherapeutic drug [147]. The nanoparticles are made of a modified dopamine (DOPA)-β-cyclodextrin (CD) combined with MnO_2-loaded nanoparticles. The surface was conjugated with the peptide tLyP-1 to increase their capacity to pass the blood brain barrier (BBB) and reach glioma cells. As expected, the MnO_2 core responded to H_2O_2 in the acidic tumor environment by releasing Mn^{2+} ions, as T_1 MRI agent and ROS generator. Moreover, the released paclitaxel also participates to the destruction of cancer cells. In another study, the coating of gold

nanorods with SiO_2 and MnO_2 enabled a shift in the optical absorbance of the nanocomposite from NIR-I to NIR-II, favoring PTT. Moreover, the released Mn^{2+} ions in the acidic environment of tumor allows a treatment with CDT. Additionally, MRI is combined with photoacoustic imaging in this nanocomposite [148]. As a last example, the recent study of Liu *et al.* [149] is very promising as it combines all the above cited therapeutic tools in the same nanoobject, composed of hollow mesoporous MnO_2 nanoparticles coated with poly(allylamine hydrochloride) (PAH) and poly(acrylic acid). These were subsequently covalently grafted with pegylated phosphorous quantum dots and then loaded with doxorubicin. In the tumor microenvironment, the structure is degraded, releasing doxorubicin and the phosphorous quantum dots as active species. Doxorubicin acts as a chemotherapeutic drug and as a fluorescence imaging agent, whereas the phosphorous quantum dots allow PDT and PTT under laser irradiation at 630 and 808 nm. Moreover, MnO_2 affords an MRI contrast, and facilitates the conversion of H_2O_2 to oxygen, enhancing PDT (figure 7).

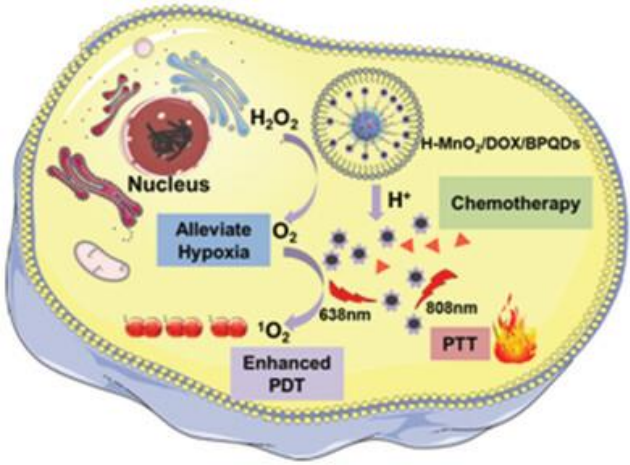

Figure 7: Illustration of the combination therapy using PTT, PDT and chemotherapy to enhance tumor treatment (reproduced with permission from [149]; copyright 5634210108465).

Toxicity Issues

All of the safety concerns raised in the previous section on nanoparticles-based MRI agents remain valid in this case. But moreover, it has to be noted that most of the above cited examples imply the release of free Mn^{2+} ions, which, as already mentioned, could induce toxicity issues, and this is not very well studied. All the in vivo studies have shown the absence of toxicity of the Mn nanoparticles at a certain concentration, suggesting low cytotoxicity and good biocompatibility, but they could become more toxic at a higher concentration. Moreover, the long-term effects of the exposure to Mn nanoparticles still have to be studied. The released Mn^{2+} ions could indeed enter the traffic routes of biological Mn, which could have latent effects. A translation to the clinic of all the above cited examples will thus require meticulous studies of their biosafety.

Conclusion

This work highlights the numerous studies performed to design highly efficient MRI contrast agents based on manganese, as a hopefully less toxic alternative to the actually used gadolinium complexes. Both molecular agents and nanoparticular agents are developed. For the first ones, relaxivities similar or higher to these of gadolinium complexes have been obtained, but a special attention to the thermodynamic stability and the kinetic inertness has to be paid. Some of the described studies are particularly interesting in that sense, so that we could hope a translation in the clinic in a near future. Concerning nanoparticular agents, their development is also very interesting since very high relaxivities can be obtained and they can be easily functionalized with different functional moieties. Meticulous toxicity studies will nevertheless be needed to translate those systems to the clinic. This is also true for theranostic agents, which are very promising to monitor and treat tumoral tissues. Hopefully the future will see the transfer to the clinic of many of these agents.

References

1. Washner J, Gale EM, Rodrigez-Rodrigez A, Caravan P. Chemistry of MRI Contrast Agents: Current Challenges and New Frontiers. Chem Rev. 2019; 119: 957-1057.
2. Iyad N, Ahmad MS, Alkhatib SG, Hjouj M. Gadolinium contrast agents- challenges and opportunities of a multidisciplinary approach: Literature review. Eur. J. Radiol. Open. 2023; 11: 100503.
3. Bauerle T, Saake M, Uder M. Gadolinium-based contrast agents: What we learned from acute adverse events, nephrogenic systemic fibrosis and brain retention. RoFo Fortschritte auf dem Gebiet der Rontgenstrahlen und der Bildgebenden Verfahren. 2021; 193: 1010-1018.
4. Martino F, Amici G, Rosner M, Ronco C, Novara G. Gadolinium-Based Contrast Media Nephrotoxicity in Kidney Impairment: The Physio-Pathological Conditions for the Perfect Murder. J. Clin. Med. 2021; 10: 271.
5. McDonald JS, McDonald RJ. MR imaging safety considerations of gadolinium-based contrast agents: gadolinium retention and nephrogenic systemic fibrosis. Magn. Reason. Imaging Clinics of North America. 2020; 28: 497-507.
6. Lancelot E, Raynaud JS, Desché P. Current and future MR contrast agents: seeking a better chemical stability and relaxivity for optimal safety and efficacy. Invest. Radiol. 2020; 55: 578-588.
7. Blomqvist L, Nordberg GF, Nurchi VM, Aaseth JO. Gadolinium in Medical Imaging—Usefulness, Toxic Reactions and Possible Countermeasures—A Review. Biomolecules. 2022; 12: 742.
8. Gianolio E, Gregorio E Di, Aime S. Chemical Insights into the Issues of Gd Retention in the Brain and Other Tissues Upon the Administration of Gd-Containing MRI Contrast Agents. Eur. J. Inorg. Chem. 2019; 2019: 137–151.
9. Chehabeddine L, Al Saleh T, Baalbaki M, Saleh E, Khoury SJ, et al. Cumulative administrations of gadolinium-based contrast agent: risks of accumulation and toxicity of linear vs macrocyclic agents. Critical Reviews in Toxicology. 2019; 49: 262-279.

10. Davies J, Siebenhandl-Wolff P, Tranquart F, Jones P, Evans P. Gadolinium: pharmacokinetics and toxicity in humans and laboratory animals following contrast agent administration. Archives of Toxicology. 2022; 96: 403-429.
11. Ali A, Shah T, Ullah R, Zhou P, Guo M, et al. Review on Recent Progress in Magnetic Nanoparticles: Synthesis, Characterization, and Diverse Applications. Front. Chem. 2021; 9.
12. Mo Y, Huang C, Liu C, Duan Z, Liu J, et al. Recent Research Progress of ^{19}F Magnetic Resonance Imaging Probes: Principle, Design, and Their Application. Macromol. Rapid Commun. 2023; 44: 2200744.
13. Akakuru OU, Iqbal MZ, Saeed M, Liu C, Paunesku T, et al. The transition from metal-based to metal-free contrast agents for T_1 magnetic resonance imaging enhancement. Bioconj. Chem. 2019; 30: 2264-2286.
14. Gupta A, Caravan P, Price WS, Platas-Iglesias C, Gale EM. Applications for transition-metal chemistry in contrast-enhanced magnetic resonance imaging. Inorg. Chem. 2020; 59: 6648-6678.
15. Wan F, Wu L, Chen X, Zhang Y, Jiang L. Research progress on manganese complexes as contrast agents for magnetic resonance imaging. Polyhedron. 2023; 242: 116489.
16. Botta M, Carniato F, Esteban-Gómez D, Platas-Iglesias C, Tei L. Mn(II) Compounds as an Alternative to Gd-Based MRI Probes. Future Med. Chem. 2019; 11: 1461–1483.
17. Crossgrove J, Zheng W. Manganese Toxicity upon Overexposure. NMR Biomed. 2004; 17: 544–553.
18. O'Neal SL, Zheng W. Manganese Toxicity Upon Overexposure: A Decade in Review. Curr Env. Health Rep. 2015; 2: 315–328.
19. Castets CR, Koonjoo N, Hertanu A, Voisin P, Franconi JM, et al. In Vivo MEMRI Characterization of Brain Metastases Using a 3D Look-Locker T1-Mapping Sequence. Sci. Rep. 2016; 6: 1–9.
20. Bianchi A, Gobbo OL, Dufort S, Sancey L, Lux F, et al. Orotracheal Manganese-Enhanced MRI (MEMRI): An Effective Approach for Lung Tumor Detection. NMR Biomed. 2017; 30: 1–10.

21. Rocklage SM, Cacheris WP, Quay SC, Hahn FE, Raymond KN. Manganese(II) N,N'-dipyridoxylethylenediamine-N,N'-diacetate 5,5'-bis(phosphate). Synthesis and characterization of a paramagnetic chelate for magnetic resonance imaging enhancement. Inorg. Chem. 1989; 28: 477-485.
22. Elizondo G, Fretz CJ, Stark DD, Rocklage SM, Quay SC, et al. Preclinical Evaluation of MnDPDP: New Paramagnetic Hepatobiliary Contrast Agent for MR Imaging. Radiology. 1991; 178: 73–78.
23. Laurent S, Vander Elst L, Muller RN. Comparative Study of the Physicochemical Properties of Six Clinical Low Molecular Weight Gadolinium Contrast Agents. Contrast Media Mol. Imaging. 2006; 1: 128–137.
24. Barandov A, Bartelle BB, Gonzales BA, White WL, Lippard SJ, et al. Membrane-permeable Mn(III) complexes for molecular magnetic resonance imaging of intracellular targets. J. Am. Chem. Soc. 2016; 138: 5483-5486.
25. Geraldes CFGC, Castro MMCA, Peters J. Mn(III) porphyrins as potential MRI contrast agents for diagnosis and MRI-guided therapy. Coord. Chem. Rev. 2021; 445: 214069.
26. Wolf GL, Burnett KR, Goldstein EJ, Joseph PM. In: Kressel H, editor. Magnetic Resonance Annual 1985. New York: Raven. 1985; 231.
27. Koenig SH, Baglin C, Brown RD, III, Brewer CF. Magnetic field dependence of solvent proton relaxation induced by Gd^{3+} and Mn^{2+} complexes Magn. Reson. Med. 1984; 1: 496-501.
28. Zhu J, Gale EM, Atanasova I, Rietz TA, Caravan P. Hexameric Mn^{II} Dendrimer as MRI Contrast Agent Chem. Eur. J. 2014; 20: 14507-14513.
29. Kálmán FK, Tircsó G. Kinetic inertness of the Mn^{2+} complexes formed with AAZTA and some open-chain EDTA derivatives. Inorg. Chem. 2012; 51: 10065–10067.
30. Borodin OY, Sannikov MY, Belyanin ML, Filimonov VD, Usov VY, et al. Relaxivity of Paramagnetic complexes of Manganese and Gadolinium. Pharm. Chem. J. 2019; 53: 635-637.

31. Gale EM, Atanasova IP, Blasi F, Ay I, Caravan P. A Manganese Alternative to Gadolinium for MRI Contrast. J. Am. Chem. Soc. 2015; 137: 15548–15557.
32. Gale EM, Wey HY, Ramsay IA, Yen YF, Sosnovik DE, et al. A manganese-based alternative to gadolinium: contrast-enhanced MR angiography, excretion, pharmacokinetics, and metabolism. Radiology. 2018; 286: 865-872.
33. Erstad DJ, Ramsay IA, Jordan VC, Sojoodi M, Fuchs BC, et al. Tumor Contrast Enhancement and Whole-Body Elimination of the Manganese-Based Magnetic Resonance Imaging Contrast Agent Mn-PyC3A. Invest. Radiol. 2019; 54: 697-703.
34. Zhou IY, Ramsay IA, Ay I, Pantazopoulos P, Rotile NJ, et al. Positron Emission Tomography–Magnetic Resonance Imaging Pharmacokinetics, In Vivo Biodistribution, and Whole-Body Elimination of Mn-PyC3A. Invest. Radiol. 2021; 56: 261-270.
35. Forgács A, Pujales-Paradela R, Regueiro-Figueroa M, Valencia L, Esteban D, et al. Platas-Iglesias. Developing the family of picolinate ligands for Mn^{2+} complexation. Dalt. Trans. 2017; 46: 1546–1558.
36. Pujales-Paradela R, Carniato F, Uzal-Varela R, Brandariz I, Iglesias E, et al. A pentadentate member of the picolinate family for Mn(ii) complexation and an amphiphilic derivative. Dalt. Trans. 2019; 48: 696–710.
37. Martinelli J, Callegari E, Baranyai Z, Fraccarollo A, Cossi M, et al. Semi-Rigid (Aminomethyl) Piperidine-Based Pentadentate Ligands for Mn(II) Complexation. Molecules. 2021; 26: 5993.
38. Bonner BP, Yurista SR, Coll-Font J, Chen S, Eder RA, et al. Contrast-Enhanced Cardiac Magnetic Resonance Imaging With a Manganese-Based Alternative to Gadolinium for Tissue Characterization of Acute Myocardial Infarction. J. Am. Heart Association. 2023; 12: e026923.
39. Cieslik P, Comba P, Dittmar B, Ndiaye D, Toth E, et al. Exceptional Manganese (II) Stability and Manganese(II)/Zinc(II) Selectivity with Rigid Polydentate Ligands. Angew. Chem. Int. Ed. 2022; 61: e202115580.
40. Anbu S, Hoffmann SHL, Carniato F, Kenning L, Price TW, et al. A single-pot template reaction towards a manganese-

based T_1 contrast agent. Angew. Chem. Int. Ed. 2021; 60: 10736-10744.
41. Drahos B, Kubicek V, Bonnet CS, Hermann P, Lukes I, et al. Dissociation Kinetics of Mn^{2+} complexes of NOTA and DOTA. Dalton Trans. 2011; 40: 1945-1951.
42. Uzal-Varela R, Rodriguez-Rodriguez A, Martinez-Calvo M, Carniato F, Lalli D, et al. Mn^{2+} complexes containing sulfonamide groups with pH-responsive relaxivity. Inorg. Chem. 2020; 59: 14306-14317.
43. Uzal-Varela R, Valencia L, Lalli D, Maneiro M, Esteban-Gomez D, et al. Understanding the effect of the electron spin relaxation on the relaxivities of Mn(II) complexes with triazacyclononane derivatives. Inorg. Chem. 2021; 60: 15055-15068.
44. Balogh E, He Z, Hsieh W, Liu S, Tóth E. Dinuclear Complexes Formed with the Triazacyclononane Derivative $ENOTA^{4-}$: High-Pressure ^{17}O NMR Evidence of an Associative Water Exchange on $[Mn^{II}_2(ENOTA)(H_2O)_2]$. Inorg. Chem. 2007; 46: 238−250.
45. Ducommun Y, Newman KE, Merbach AE. High-pressure oxygen-17 NMR evidence for a gradual mechanistic changeover from Ia to Id for water exchange on divalent octahedral metal ions going from manganese(II) to nickel(II). Inorg. Chem. 1980; 19: 3696-3703.
46. Patinec V, Rolla GA, Botta M, Tripier R, Esteban-Gomez D, et al. Hyperfine Coupling Constants on Inner-Sphere Water Molecules of a Triazacyclononane-based Mn(II) Complex and Related Systems Relevant as MRI Contrast Agents. Inorg. Chem. 2013; 52: 11173-11184.
47. de Sá A, Bonnet CS, Geraldes CFGC, Tóth E, Ferreira PMT, et al. Thermodynamic stability and relaxation studies of small, triaza-macrocyclic Mn(ii) chelates. Dalton Trans. 2013; 42: 4522-4532.
48. Pujales-Paradela R, Carniato F, Esteban-Gomez D, Botta M, Platas-Iglesias C. Controlling water exchange rates in potential Mn^{2+}-based MRI agents derived from NO_2A^{2-}. Dalton Trans. 2019; 48: 3962-3972.
49. Rolla GA, Platas-Iglesias C, Botta M, Tei L, Helm L. ^1H and ^{17}O NMR Relaxometric and Computational Study on

Macrocyclic Mn(II) Complexes. Inorg. Chem. 2013; 52: 3268-3279.
50. Garda Z, Forgacs A, Do QN, Kalman FK, Timari S, et al. Physico-chemical properties of Mn^{II} complexes formed with cis- and trans-DO2A: thermodynamic, electrochemical and kinetic studies. J. Inorg. Biochem. 2016; 163: 206-213.
51. Forgacs A, Tei L, Baranyai Z, Toth I, Zekany L, et al. A Bisamide Derivative of [Mn(1,4-DO2A)] – Solution Thermodynamic, Kinetic, and NMR Relaxometric Studies. Eur. J. Inorg. Chem. 2016; 1165-1174.
52. Garda Z, Molnár E, Kálmán FK, Botár R, Nagy V, et al. Effect of the Nature of Donor Atoms on the Thermodynamic, Kinetic and Relaxation Properties of Mn(II) Complexes Formed with Some Trisubstituted 12-Membered Macrocyclic Ligands. Front. Chem. 2018; 6: 1–14.
53. Tei L, Gugliotta G, Fekete M, Kalman FK, Botta M. Mn(II) complexes of novel hexadentate AAZTA-like chelators: a solution thermodynamics and relaxometric study. Dalton Trans. 2011; 40: 2025-2032.
54. Garda Z, Molnar E, Hamon N, Barriada JL, Esteban-Gomez D, et al. Complexation of Mn(II) by Rigid Pyclen Diacetates: Equilibrium, Kinetic, Relaxometric, Density Functional Theory, and Superoxide Dismutase Activity Studies. Inorg. Chem. 2021; 60: 1133-1148.
55. Devreux M, Henoumont C, Dioury F, Boutry S, Vacher O, et al. Mn^{2+} complexes with Pyclen-based derivatives as contrast agents for magnetic resonance imaging: synthesis and relaxometry characterization. Inorg. Chem. 2021; 60: 3604-3619.
56. Drahoš B, Kotek J, Cíśarŏvá I, Hermann P, Helm L, et al. Mn^{2+} Complexes with 12-Membered Pyridine Based Macrocycles Bearing Carboxylate or Phosphonate Pendant Arm: Crystallographic, Thermodynamic, Kinetic, Redox, and 1H/17O Relaxation Studies. Inorg. Chem. 2011; 50: 12785–12801.
57. Drahos B, Kotek J, Hermann P, Lukes I, Toth E. Mn^{2+} Complexes with Pyridine-Containing 15-Membered Macrocycles: Thermodynamic, Kinetic, Crystallographic, and $^{1}H/^{17}O$ Relaxation Studies. Inorg. Chem. 2010; 49: 3224-3238.

58. Pota K, Molnar E, Kalman FK, Freire DM, Tircso G, et al. Manganese Complex of a Rigidified 15-Membered Macrocycle: A Comprehensive Study. Inorg. Chem. 2020; 59: 11366-11376.
59. Prazakova M, Ndiaye D, Toth E, Drahos B. A seven-coordinate Mn(II) complex with a pyridine-based 15-membered macrocyclic ligand containing one acetate pendant arm: structure, stability and relaxation properties. Dalton Trans. 2023; 52: 7936-7947.
60. Nagendraraj T, Kumaran SS, Mayilmurugan R. Mn(II) complexes of phenylenediamine based macrocyclic ligands as T_1-MRI contrast agents. J. Inorg. Biochem. 2022; 228: 111684-111692.
61. Reale G, Calderoni F, Ghirardi T, Porto F, Illuminati F, et al. Development and evaluation of the magnetic properties of a new manganese (II) complex: a potential MRI contrast agent. Int. J. Mol. Sci. 2023; 24: 3461.
62. Uzal-Varela R, Perez-Fernandez F, Valencia L, Rodriguez-Rodriguez A, Platas-Iglesias C, et al. Thermodynamic stability of Mn(II) complexes with aminocarboxylate ligands analyzed using structural descriptors. Inorg. Chem. 2022; 61: 14173-14186.
63. Islam MK, Kim S, Kim HK, Park S, Lee GH, et al. Manganese Complex of Ethylenediaminetetra acetic acid (EDTA)-Benzothiazole Aniline (BTA) Conjugate as a Potential Liver-Targeting MRI Contrast Agent. J. Med. Chem. 2017; 60: 2993-3001.
64. Islam MK, Kim S, Kim HK, Kim YH, Lee YM, et al. Synthesis and Evaluation of Manganese (II)-based Ethylenediaminetetraacetic Acid-Ethoxybenzyl Conjugate as a Highly Stable Hepatobiliary Magnetic Resonance Imaging Contrast Agent. Bioconjug. Chem. 2018; 29: 3614.
65. McRae SW, Cleary M, DeRoche D, Martinez FM, Xia Y, et al. Development of a Suite of Gadolinium-Free OATP1-Targeted Paramagnetic Probes for Liver MRI. J. Med. Chem. 2023; 66: 6567-6576.
66. Hall RC, Qin J, Laney V, Ayat N, Lu ZR. Manganese(II) EOB-Pyclen Diacetate for Liver-Specific MRI. ACS Appl. Bio. Mater. 2022; 5: 451-458.

67. Islam MK, Baek MK, Yang AR, Kim BW, Hwang S, et al. Manganese (II) Complex of 1,4,7-Triazacyclononane-1,4,7-Triacetic Acid (NOTA) as a Hepatobiliary MRI Contrast Agent. Pharmaceuticals. 2023; 16: 602.
68. Wang J, Wang H, Ramsay IA, Erstad DJ, Fuchs BC, et al. Manganese-Based Contrast Agents for Magnetic Resonance Imaging of Liver Tumors: Structure Activity Relationships and Lead Candidate Evaluation. J. Med. Chem. 2018; 61: 8811-8824.
69. Chen K, Li P, Zhu C, Xia Z, Xia Q, et al. Mn(II) Complex of Lipophilic Group-Modified Ethylenediaminetetraacetic Acid (EDTA) as a New Hepatobiliary MRI Contrast Agent. J. Med. Chem. 2021; 64: 9182-9192.
70. Xue Y, Xiao B, Xia Z, Dai L, Xia Q, et al. A New OATP-mediated hepatobliliary-specific Mn(II)-based MRI contrast agent for hepatocellular carcinoma in mice: a comparison with Gd-EOB-DTPA. J. Magn. Reson. Imaging. 2023; 58: 926-933.
71. Ning Y, Zhou IY, Rotile NJ, Pantazopoulos P, Wang H, et al. Dual Hydrazine-Equipped Turn-On Manganese-Based Probes for Magnetic Resonance Imaging of Liver Fibrogenesis. J. Am. Chem. Soc. 2022; 144: 16553-16558.
72. Aime S, Anelli PL, Botta M, Brocchetta M, Canton S, et al. Relaxometric evaluation of novel manganese(III) complexes for application as contrast agents in magnetic resonance imaging. J. Biol. Inorg. Chem. 2002; 7: 58-67.
73. Troughton JS, Greenfield MT, Greenwood JM, Dumas S, Wiethoff AJ, et al. Synthesis and Evaluation of a High Relaxivity Manganese(II)-Based MRI Contrast Agent. Inorg. Chem. 2004; 43: 6313-6323.
74. Baroni S, Serra SC, Mingo AF, Lux G, Giovenzana GB, et al. Synthesis and Relaxometric Characterization of a New Mn(II)-EDTA-Deoxycholic Acid Conjugate Complex as a Potential MRI Blood Pool Agent. Chem. Select. 2016; 1: 1607-1612.
75. Kalman FK, Nagy V, Varadi B, Garda Z, Molnar E, et al. Mn(II)-based MRI contrats agent candidate for vascular imaging. J. Med. Chem. 2020; 63: 6057.
76. Forgacs A, Tei L, Baranyai Z, Esteban-Gomez D, Platas-Iglesias C, et al. Optimising the relaxivities of

Mn^{2+} complexes by targeting human serum albumin (HSA). Dalton Trans. 2017; 46: 8494-8504.
77. Leone L, Anemone A, Carella A, Botto E, Longo DL, et al. A neutral and stable macrocyclic Mn(II) complex for MRI tumor visualization. ChemMedChem. 2022; 17: e202200508.
78. Zhou Z, Bai R, Wang Z, Bryant H, Lang L, et al. An albumin-binding T_1-T_2 dual-modal MRI contrast agents for improved sensitivity and accuracy in tumor imaging. Bioconj. Chem. 2019; 30: 1821-1829.
79. Forgacs A, Regueiro-Figueroa M, Barriada JL, Esteban-Gomez D, de Blas A, et al. Mono-, Bi-, and Trinuclear Bis-Hydrated Mn^{2+} Complexes as Potential MRI Contrast Agents. Inorg. Chem. 2015; 54: 9576.
80. Su H, Wu C, Zhu J, Miao T, Wang D, et al. Rigid Mn(II) chelate as efficient MRI contrast agent for vascular imaging. Dalton Trans. 2012; 41: 14480.
81. Rolla G, De Biasio V, Giovenzana GB, Botta M, Tei L. Supramolecular assemblies based on amphiphilic Mn^{2+}-complexes as high relaxivity MRI probes. Dalton Trans. 2018; 47: 10660-10670.
82. Mulas G, Rolla GA, Geraldes CFGC, Starmans LWE, Botta M, et al. Mn(II)-Based Lipidic Nanovesicles as High-Efficiency MRI Probes. ACS Appl. Bio. Mater. 2020; 3: 2401-2409.
83. Liu X, Fu S, Xia C, Li M, Cai Z, et al. PEGylated amphiphilic polymeric manganese(II) complexes as magnetic resonance angiographic agents. J. Mater. Chem. B 2022; 10: 2204-2214.
84. Chen K, Cai Z, Cao Y, Jiang L, Jiang Y, et al. Kinetically inert manganese (II)-based hybrid micellar complexes for magnetic resonance imaging of lymph node metastasis. Regenerative Biomater. 2023; 10: rbad053.
85. Swietach P, Vaughan-Jones RD, Harris AL, Hulikova A. The chemistry, physiology, and pathology of pH in cancer. Philos. Trans. R. Soc. B Biol. Sci. 2014; 369: 20130099.
86. Botar R, Molnar E, Trencsenyi G, Kiss J, Kalman FK, et al. Stable and inert Mn(II)-based and pH responsive contrast agents. J.Am. Chem. Soc. 2020; 142: 1662.

87. Shen X, Pan Y, Liang G. Development of macrocyclic Mn(II)-Bispyridine complexes as pH responsive magnetic resonance imaging contrast agents. Eur. J. Inorg. Chem. 2023; 26: e202200786.
88. Loving GS, Mukherjee S, Caravan P. Redox-activated manganese-based MR contrast agent. J. Am. Chem. Soc. 2013; 135: 4620-4623.
89. Gale ME, Mukherjee S, Liu C, Loving GS, Caravan P. Structure-redox-relaxivity relationships for redox responsive manganese-based magnetic resonance imaging probes. Inorg. Chem. 2014; 53: 10748-10761.
90. Gale EM, Jones CM, Ramsay I, Farrar CT, Caravan P. A Janus Chelator Enables Biochemically Responsive MRI Contrast with Exceptional Dynamic Range. J. Am. Chem. Soc. 2016; 138: 15861-15864.
91. Yu M, Beyers RJ, Gorden JD, Cross JN, Goldsmith CR. A Magnetic Resonance Imaging Contrast Agent Capable of DetectingHydrogen Peroxide. Inorg. Chem. 2012; 51: 9153-9155.
92. Yu M, Ambrose SL, Whaley ZL, Fan S, Gorden JD, et al. A Mononuclear Manganese(II) Complex Demonstrates a Strategy ToSimultaneously Image and Treat Oxidative Stress. J. Am. Chem. Soc. 2014; 136: 12836-12839.
93. Li Y, Xia Q, Zhu C, Cao W, Xia Z, et al. An activatable Mn(II) MRI probe for detecting peroxidase activity in vitro and in vivo. J. Inorg. Biochem. 2022; 236: 111979.
94. Botar R, Molnar E, Garda Z, Madarasi E, Trencsenyi G, et al. Synthesis and characterization of a stable and inert Mn^{II}-based Zn^{II} responsive MRI probe for molecular imaging of glucose stimulated zinc secretion (GSZS). Inorg. Chem. Front. 2022; 9: 577-583.
95. Vitor T, Martins KM, Ionescu TM, Cunha ML, Baroni RH, et al. PET/MRI: a novel hybrid imaging technique. Major clinical indications and preliminary experience in Brazil. Einstein Sao Paulo. 2017; 15: 115-118.
96. Vanasschen C, Monar E, Tircso G, Kalman FK, Toth E, et al. Inorg. Chem. 2017; 56: 7746.
97. Csupasz T, Szücs D, Kalman FK, Holloczki O, Fekete A, et al. A new oxygen containing pyclen-type ligand as a manganese(II) binder for MRI and ^{52}Mn PET applications:

equilibrium, kinetic, relaxometric, structural and radiochemical studies. Molecules. 2022; 27: 371.

98. Sathiyajith C, Hallett AJ, Edwards PG. Synthesis, photophysical characterization, relaxometric studies and molecular docking studies of gadolinium-free contrast agents for dual modal imaging. Results in Chemistry. 2022; 4: 100307.
99. Feng Z, Zhu T, Wang L, Yuan T, Jiang Y, et al. Coordination-Regulated Terpyridine–Mn(II) Complexes for Photodynamic Therapy Guided by Multiphoton Fluorescence/Magnetic Resonance Imaging. Inorg. Chem. 2022; 61: 12652-12661.
100. Tan M, Wu X, Jeong EK, Chen Q, Parker DL, et al. An effective targeted nanoglobular manganese(II) chelate conjugate for magnetic resonance molecular imaging of tumor extracellular matrix. Mol. Pharm. 2010; 7: 936-943.
101. Tan M, Ye Z, Jeong EK, Wu X, Parker DL, et al. Synthesis and evaluation of nanoglobular macrocyclic Mn(II) chelate conjugates as non-gadolinium(III) MRI contrast agents. Bioconj. Chem. 2011; 22: 931-937.
102. Sun C, Lin H, Gong X, Yang Z, Mo Y, et al. DOTA-branched organic frameworks as giant and potent metal chelators. J. Am. Chem. Soc. 2020; 142: 198-206.
103. Sun C, Yang Z, Wu P, Luo X, Liu K, et al. Multinuclear Mn(II) united-DOTA complexes with enhanced inertness and high MRI contrast ability. Cell Reports Phys. Science. 2022; 3: 100920.
104. Carniato F, Ricci M, Tei L, Garello F, Furlan C, et al. Novel nanogels loaded with Mn(II) chelates as effective and biologically stable MRI probes. Small. 2023; 2302868.
105. Mallik R, Saha M, Mukherjee C. Porous Silica Nanospheres with a Confined Mono(aquated) Mn(II)-Complex: A Potential T_1–T_2 Dual Contrast Agent for Magnetic Resonance Imaging. ACS Appl. Bio. Mater. 2021; 4: 8356-8367.
106. Eriksson PO, Aaltonen E, Petoral Jr, R, Lauritzson P, Miyazaki H, et al. Novel Nano-Sized MR Contrast Agent Mediates Strong Tumor Contrast Enhancement in an Oncogene-Driven Breast Cancer Model. PLoS ONE. 2014; 9: e107762.

107. Gianolio E, Bäckström S, Petoral Jr, RM, Olsson A, Aime S, et al. Characterization of a Manganese-Containing Nanoparticle as an MRI Contrast Agent. Eur. J. Inorg. Chem. 2019; 13: 1759-1766.
108. Palmai M, Petho A, Nagy LN, Klébert S, May Z, et al. Direct immobilization of manganese chelates on silica nanospheres for MRI applications. J. Colloid Interface Sci. 2017; 498: 298-305.
109. Lalli D, Ferrauto G, Terreno E, Carniato F, Botta M. Mn(II)-conjugated silica nanoparticles as potential MRI probes. J. Mater. Chem. B 2021; 9: 8994.
110. Farinha P, Coelho JMP, Reis CP, Gaspar MM. A Comprehensive Updated Review on Magnetic Nanoparticles in Diagnostics. Nanomaterials. 2021; 11: 3432.
111. Caspani S, Magalhaes R, Araujo JP, Sousa CT. Magnetic Nanomaterials as Contrast Agents for MRI. Materials. 2020; 13: 2586.
112. Cai X, Zhu Q, Zeng Y, Zeng Q, Chen X, et al. Manganese oxide nanoparticles as MRI contrast agents in tumor multimodal imaging and therapy. Int. J. Nanomedicine. 2019; 14: 8321-8344.
113. Hashemzadeh S, Akbari ME, Astani SA, Hashemzadeh J, Hafez AA. Engineering effects on efficacy and toxicity of manganese oxide nanostructures, as a contrast agent, in magnetic resonance imaging: A review. Nano. 2022; 17: 2230003.
114. Zhen Z, Xie J. Development of manganese-based nanoparticles as contrast probes for magnetic resonance imaging. Theranostics. 2012; 2: 45-54.
115. Li J, Wu C, Hou P, Zhang M, Xu K. One-pot preparation of hydrophilic manganese oxide nanoparticles as T1 nano-contrast agent for molecular magnetic resonance imaging of renal carcinoma in vitro and in vivo. Biosens. Bioelectron. 2018; 102: 1-8.
116. Huang HT, Yue T, Xu K, Golzarian J, Yu JH, et al. Fabrication and evaluation of tumor-targeted positive MRI contrast agent based on ultrasmall MnO nanoparticles. Colloid Surf. B. 2015; 131: 148-154.
117. Huang HT, Yue T, Xu YY, Xu K, Xu H, et al. PEGylation of MnO nanoparticles via catechol-Mn chelation

to improving T_1 weighted magnetic resonance application. J. Appl. Polym. Sci. 2015; 132: 42360.

118. Hsu BYW, Wang M, Zhang Y, Vijayaragavan V, Wong SY, et al. Silica-F127 nanohybrid-encapsulated manganese oxide nanoparticles for optimized T1 magnetic resonance relaxivity. Nanoscale. 2014; 6: 293-299.

119. Costanzo M, Scolaro L, Berlier G, Marengo A, Grecchi S, et al. Cell uptake and intracellular fate of phospholipidic manganese-based nanoparticles. Int. J. Pharmaceut. 2016; 508: 83-91.

120. Gallo J, Alam IS, Lavdas I, Wylezinska-Arridge M, Aboagye EO, et al. RGD-targeted MnO nanoparticles as T1 contrast agents for cancer imaging – the effect of PEG length in vivo. J. Mater. Chem. B. 2014; 2: 868-876.

121. Peng YK, Lui CNP, Chen YW, Chou SW, Raine E, et al. Engineering of single magnetic particle carrier for living brain cell imaging: a tunable T1/T2 dual-modal contrast agent for magnetic resonance imaging application. Chem. Mater. 2017; 29: 4411-4417.

122. Peng E, Wang FH, Tan SH, Zheng BW, Li SFY, et al. Tailoring a two-dimensional graphene-oxide surface: dual T1 and T2 MRI contrast agent materials. J. Mater. Chem. B. 2015; 3: 5678-5682.

123. Zheng YY, Zhang H, Hu YP, Bai L, Xue JY. MnO nanoparticles with potential application in magnetic resonance imaging and drug delivery for myocardial infarction. Int. J. Nanomed. 2018; 13: 6177-6188.

124. Chen N, Shao C, Li S, Wang Z, Qu Y, et al. Cy5.5 conjugated MnO nanoparticles for magnetic resonance/near-infrared fluorescence dual-modal imaging of brain gliomas. J. Colloid Interf. Sci. 2015; 457: 27-34.

125. Paul G, Prado Y, Dia N, Rivière E, Laurent S, et al. Mn^{II}-containing coordination nanoparticles as highly efficient T1 contrast agents for magnetic resonance imaging. Chem. Commun. 2014; 50: 6740-6743.

126. Panich AM, Shames AI, Aleksenskii AE, Yudina EB, Vul A. Ya. Manganese-grafted detonation nanodiamond, a novel potential MRI contrast agent. Diam. Relat. Mater. 2021; 119: 108590.

127. Panich AM, Salti M, Aleksenskii AE, Kulvelis YV, Chizhikova A, et al. Suspensions of manganese-grafted nanodiamonds: preparation, NMR, and MRI study. Diam. Relat. Mater. 2023; 131: 109591.
128. Qin R, Li S, Qiu Y, Feng Y, Liu Y, et al. Carbonized paramagnetic complexes of Mn(II) as contrast agents for precise magnetic resonance imaging of sub-millimeter-sized orthotopic tumors. Nature Commun. 2022; 13: 1938.
129. Stepanidenko EA, Vedernikova AA, Badrieva ZF, Brui EA, Ondar SO, et al. Manganese-doped carbon dots as a promising nanoprobe for luminescent and magnetic resonance imaging. Photonics. 2023; 10: 757.
130. Huang X, Wang Z, Li S, Lin S, Zhang L, et al. Non-invasive diagnosis of acute kidney injury using Mn-doped carbon dots-based magnetic resonance imaging. Biomater. Science. 2023; 11: 4289-4297.
131. Zhang Y, Liu L, Li W, Zhang C, Song T, et al. PDGFB-targeted functional MRI nanoswitch for activatable T_1-T_2 dual-modal ultra-sensitive diagnosis of cancer. J. Nanobiotech. 2023; 21: 9.
132. Iki N, Nakane R, Masuya-Suzuki A, Ozawa Y, Maruoka T, et al. MRI contrasting agent based on Mn-MOF-74 nanoparticles with coordinatively unsaturated sites. Mol. Imaging Biol. 2023.
133. Sun M, Chen G, Ouyang S, Chen C, Zheng Z, et al. Magnetic Resonance Diagnosis of Early Triple-Negative Breast Cancer Based on the Ionic Covalent Organic Framework with High Relaxivity and Long Retention Time. Anal. Chem. 2023; 95: 8267-8276.
134. Tullio C, Salvioni L, Bellini M, Degrassi A, Fiandra L, et al. Development of an effective tumor-targeted contrast agent for magnetic resonance imaging based on Mn/H-ferritin. ACS Appl. Bio Mater. 2021; 4: 7800-7810.
135. Pashkunova-Martic I, Kukeva R, Stoyanova R, Pantcheva I, Dorkov P, et al. Novel salinomycin-based paramagnetic complexes – First evaluation of their potential theranostic properties. Pharmaceutics. 2022; 14: 2319.
136. Antwi-Baah R, Wang Y, Chen X, Liu H, Yu K. Hybrid morphologies of paramagnetic manganese-based

nanoparticles as theranostics. Chem. Engineering J. 2023; 466: 142970.
137. Liu X, Rong P. Recent advances of manganese-based hybrid nanomaterials for cancer precision medicine. Frontiers in oncology. 2021; 11: 707618.
138. Zheng R, Guo J, Cai X, Bin L, Lu C, et al. Manganese complexes and manganese-based metal-organic frameworks as contrast agents in MRI and chemotherapeutics agents: applications and prospects. Colloids and surfaces B: biointerfaces. 2022; 213: 112432.
139. Babaei M, Abnous K, Nekooei S, Taghdisi SM, Farzad SA, et al. Synthesis of manganese-incorporated polycaprolactone-poly (glyceryl methacrylate) theranostic smart hybrid polymersomes for efficient colon adenocarcinoma treatment. Int. J. Pharm. 2022; 623: 121963.
140. Ma H, Zhang X, Pang L, Yu B, Cong H, et al. Mn-dox metal-organic nanoparticles for cancer therapy and magnetic resonance imaging. Dyes and pigments. 2022; 199: 110080.
141. Arkaban H, Shervedani RK, Torabi M, Norouzi-Barough L. Fabrication of a biocompatible and biodegradable targeted theranostic nanocomposite with pH-controlled drug release ability. J. of Drug Delivery Science and Technology. 2022; 72: 103403.
142. Jiang G, Fan D, Tian J, Xiang Z, Fang Q. Self-confirming magnetosomes for tumor-targeted T_1/T_2 dual-mode MRI and MRI-guided photothermal therapy. Adv. Healthcare Mater. 2022; 11: 2200841.
143. Shen Y, Li X, Huang H, Lan Y, Gan L, et al. Embedding Mn^{2+} in polymer coating on rod-like cellulose nanocrystal to integrate MRI and photothermal function. Carbohydrate Polymers. 2022; 297: 120061.
144. Li M, Huo L, Zeng J, Zhu G, Liu X, et al. Switchable ROS scavenger/generator for MRI-guided anti-inflammation and anti-tumor therapy with enhanced therapeutic efficacy and reduced side effects. Adv. Healthcare Mater. 2023; 12: 2202043.
145. Rehman ZU, Iqbal MZ, Hou J, Butt FK, AlFaify S, et al. Graphitic carbon nitride-manganese oxide nanoflowers as promising T1 magnetic resonance imaging contrast material. Appl. Phys. A. 2022; 128: 926.

146. Wang H, Bremner DH, Wu K, Gong X, Fan Q, et al. Platelet membrane biomimetic bufalin-loaded hollow MnO2 nanoparticles for MRI-guided chemo-chemodynamic combined therapy of cancer. Chem. Eng. J. 2020; 382: 122848.
147. Jiang S, Li X, Zhang F, Mao J, Cao M, et al. Manganese dioxide-based nanocarrier delivers Paclitaxel to enhance chemotherapy against orthotopic glioma through hypoxia relief. Small Methods. 2022; 2101531.
148. He T, Jiang G, He J, Zhang Y, He G, et al. Manganese-dioxide-coating-instructed plasmonic modulation of gold nanorods for activatable duplex-imaging-guided NIR-II photothermal-chemodynamic therapy. Adv. Mater. 2021; 33: 2008540.
149. Wu Y, Chen Z, Yao Z, Zhao K, Shao F, et al. Black Phosphorus Quantum Dots Encapsulated Biodegradable Hollow Mesoporous MnO_2: Dual-Modality Cancer Imaging and Synergistic Chemo-Phototherapy. Adv. Funct. Mater. 2021; 31: 2104643.